JOC The Journal of Organic Chemistry

Subscriber access provided by UNIVERSITY OF BRIGHTON

Article

Synthesis of Flavonols via Pyrrolidine Catalysis: Origins of the Selectivity for Flavonol versus Aurone

Wei Xiong, Xiaohong Wang, Xianyan Shen, Cuifang Hu, Xin Wang, Fei Wang, Guolin Zhang, and Chun Wang

J. Org. Chem., **Just Accepted Manuscript** • DOI: 10.1021/acs.joc.0c01869 • Publication Date (Web): 24 Sep 2020

Downloaded from pubs.acs.org on September 27, 2020

Just Accepted

"Just Accepted" manuscripts have been peer-reviewed and accepted for publication. They are posted online prior to technical editing, formatting for publication and author proofing. The American Chemical Society provides "Just Accepted" as a service to the research community to expedite the dissemination of scientific material as soon as possible after acceptance. "Just Accepted" manuscripts appear in full in PDF format accompanied by an HTML abstract. "Just Accepted" manuscripts have been fully peer reviewed, but should not be considered the official version of record. They are citable by the Digital Object Identifier (DOI®). "Just Accepted" is an optional service offered to authors. Therefore, the "Just Accepted" Web site may not include all articles that will be published in the journal. After a manuscript is technically edited and formatted, it will be removed from the "Just Accepted" Web site and published as an ASAP article. Note that technical editing may introduce minor changes to the manuscript text and/or graphics which could affect content, and all legal disclaimers and ethical guidelines that apply to the journal pertain. ACS cannot be held responsible for errors or consequences arising from the use of information contained in these "Just Accepted" manuscripts.

is published by the American Chemical Society. 1155 Sixteenth Street N.W., Washington, DC 20036

Published by American Chemical Society. Copyright © American Chemical Society. However, no copyright claim is made to original U.S. Government works, or works produced by employees of any Commonwealth realm Crown government in the course of their duties.

Synthesis of Flavonols via Pyrrolidine Catalysis: Origins of the Selectivity for Flavonol versus Aurone

Wei Xiong,[†,‡,∥] Xiaohong Wang,[†,‡,∥] Xianyan Shen,[†,‡] Cuifang Hu,[§] Xin Wang,[§] Fei Wang,[†] Guolin Zhang,[†,*] and Chun Wang[†,*]

[†] Chengdu Institute of Biology, Chinese Academy of Sciences, Chengdu 610041, China

[‡] University of Chinese Academy of Sciences, Beijing 100049, China

[§] College of Chemistry, Sichuan University, Chengdu 610064, China

* E-mail: wangchun@cib.ac.cn, Zhanggl@cib.ac.cn

Supporting Information Place hold

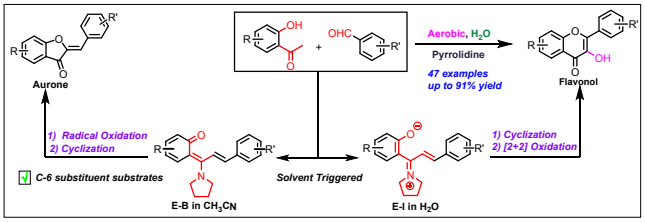

ABSTRACT: A novel synthetic method for flavonol from 2'-hydroxyl acetophenone and benzaldehyde promoted by pyrrolidine under an aerobic condition in water is established. This protocol was supported by efficient synthesis of 44 common examples and three natural products. The *α*, *β*-unsaturated iminium ion (enimine ion **E**) was proved to be the key intermediate in the reaction. $H_2{}^{18}O$ and ${}^{18}O_2$ isotope tracking experiments demonstrated that both water and the aerobic atmosphere were necessary to ensure the transformation. The selectivity for flavonol or aurone was originated from solvent triggered intermediates, which were determined by UV-visible spectra from isolated enimine. The phenol-iminium **E-A** is dominant in water and the ketoenamine intermediate **E-B** is prevalent in acetonitrile. Under the presence of pyrrolidine and oxygen, **E-A** leads to flavonol through **E-I**, a zwitterionic-like phenoloxyl-iminium ion, following the key steps of cyclization and a [2+2] oxidation; and **E-B** proceeds through Path II, a radical process induced by photolysis of **E-B** with both pyrrolidine and oxygen, to afford aurone. Preliminary mechanistic studies are reported.

■ INTRODUCTION

Flavonols (3-hydroxyflavones) are distributed widely in plant kingdom and exist in a wide variety of natural plants. Besides their plant physiological importance, they attract considerable interest due to their biological effects, including antiviral, antitumor and antibiotic activities.[1] Most of the natural occurring flavonols with therapeutic significance contain substituents at *C-5*. For example, quercetin and kaempferol distinctly inhibit cancer cell lipogenesis in both prostate and breast cancer cells.[2] Icaritin inhibits malignant growth of hepatocellular carcinoma-initiating cells (HCICs) and may potentially be developed into an effective therapeutic agent for the treatment of hepatocellular carcinoma (HCC).[3] The senolytic cocktail, dasatinib plus quercetin, can selectively eliminate senescent cells and enhance remaining health and lifespain in old mice.[4] In spite of the biological importance of flavonols, limited synthetic methods available include those with key reactions such as Algar-Flynn-Oyamada (AFO) reaction,[5] Baker-Venkataraman rearrangement[6] Auwers[7] and dimethyldioxirane (DMDO) Oxidation.[8] In addition to tedious synthetic processes, harmful oxidants and solvents are also involved. More vitally, these methods are not efficient for the generation of *C-5* substituted flavonols. The AFO reaction is the most adapted method for synthesis of flavonols, which is through the reaction of 2'-hydroxychalcone with alkaline hydrogen peroxide. The major by-product aurone in the synthesis of 5-substituted flavonol has been accounted for the 6'-substituent directed cyclisation of phenolate in the postulated chalcone epoxide intermediate to C-*α* rather than C-*β* of the carbonyl group.[9] By using weaker bases, such as sodium carbonate, the yields of *C-5* substituted flavonols could be moderately increased. The over-oxidized by-products in the presence of hydrogen

peroxide are still unavoidable.

In terms of AFO reaction, two key steps are involved in the transformation from 2'-hydroxylacetophenone and benzaldehyde into flavonol, the aldol condensation (formation of chalcone) and oxidative cyclization. Thus, a base (either inorganic alkali, Scheme 1 (a) or amine, Scheme 1 (b)) and an oxidant would be necessary. When we intended to use pyrrolidine as base to catalyze the aldol condensation of 2'-hydroxy-6'- methoxyaceto-

Scheme 1. Analysis of the formation of flavonol from acetophenone and benzaldehyde: a) Through chalcone; b) through iminium activation

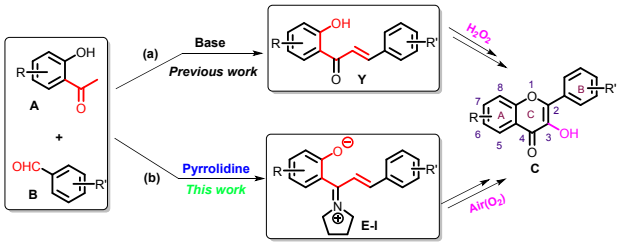

phenone and 4-methoxybenzaldehyde under an aerobic condition in methanol, we founded surprisingly that flavonol came out as the major product whereas aurone was detected as minor product.

In addition, we confirmed the formation of iminium-ion intermediate (**E_1**; R=6'-OMe; R'=4-OMe) in the model reaction by *in situ* ^{1}H NMR measurement. Thus, we may reasonably assume that the pyrrolidine not only worked as a base for catalyzing the aldol condensation, but also activated the *α*, *β*-unsaturated ketone through the formation of iminium-ion. The latter was converted into flavonol and aurone involving oxidation by reactive oxygen species (ROS) from the environment (air). The formation of iminium-ion is known as the LUMO activation in amino catalysis, which represents an important class of powerful and straightforward approach for the construction of complex molecules in a very efficient way.[10] Many reactions are involved in amino catalysis such as Michael reaction,[11] [2+2] cyclization,[12] Diels-Alder reaction,[13] and singel-electron transfer (SET) reaction.[14] Oxidative reaction of the enimine ion or enamine is less known, except the epoxidation of enimine with hydrogen peroxide.[15] To the best of our knowledge, the oxidation of enimine catalysed by secondary amine under aerobic condition remains unexplored.

The generation and properties of ROS are of great interest in organic chemistry. It is well known that O_2 can be photoactivated through type I and type II processes to generate reactive oxygen species (ROS).[16] Type I undergoes photoinduced electron transfer to form O_2^{-} and $HO_2^{\cdot}$, consequently, a radical process is involved. Type II is a sensitizer energy-transfer process to oxygen involved the formation of singlet oxygen ($^1O_2$). Despite the types of ROS exhibite varying lifetimes in different media, the rate of oxygenated product formation can also vary widely; for example, the rate constant for the reaction of methionine with $^1O_2$ is ~60 mollion-fold greater than that with O_2^{-}.[17]. Although the use of ROS to synthesize natural products are coming into use, [18] controlling of the types of ROS reaction is still challenging and its use for manipulating the products selectivity is not known.

As part of our ongoing program on the methodology development and mechnism implication of natural flavonol synthesis, we have exploited the selective synthesis of flavonols catalysized by pyrrolidine. Although Cao et al. described a synthesis of flavonol from benzaldehyde and 2'-hydroxylacetophenone in the existence of pyrrolidine in ethanol,[19] the scope and the mechanism of reaction were not disclosed. Our preliminary experimental results show that 1) air is necessary for the reaction, 2) flavonols were generated with poor selectivity in ethanol. However, we found that the reaction could be preferentially directed to flavonol by using water as solvent. On the other hand, by switching the solvent to acetonitrile under otherwise identical conditions would favor the generation of aurone. 3) aurone was inhibited by addition of TEMPO, in the meantime, generation of flavonol was not influenced. which indicated that two different pathways were involved, in which one was a non-radical pathway and the other was a radical pathway. Motivated by this intriguing selectivity disparity, and the likely interplay of the directing solvent influence to the selectivity, a systematic study on the reaction and mechanism was carried out to reveal the origin for the selectivity of flavonol versus aurone, and to delineate the structural features of substrates responsible for the reaction. We wish that our findings can reveal new and fascinating reaction of *α*, *β*-unsaturated enamines or enimine salts.

RESULTS AND DISCUSSION

The reaction of 2'-hydroxy-6'-methoxyacetophenone (**A_1**) and 4-methoxybenzaldehyde (**B_1**) was taking as the model reaction, primary, secondary and tertiary amines were screened for the synthesis of flavonols (Table 1). The reaction was promoted by cyclic secondary amines. Piperidine is poorer than pyrrolidine (Table 1, Entry 4, 5). Among the amines screened, pyrrolidine provided the maximum yield of flavonol. Open-chain primary, secondary and tertiary amines were unable to accomplish the reaction and the reaction remained at flavonone step (Table 1, Entry 1, 2, 8). Strong base like TBD resulted in chalcone (Table 1, Entry 7). Next, we optimized the amount of pyrrolidine. Reducing the equivalents of pyrrolidine from 10 to 4 resulted in slow down of the reaction and reduced yield of **C_1**. When 2-4 equivalents of pyrrolidine were used, the reaction was extremely slow. On the other hand, further increasing the amount of pyrrolidine to above 10 equivalents had no obvious influence on the reaction speed and the yield of flavonols. Thus, the optimal amount of pyrrolidine was found to be 10 equivalents. The effect of the solvent was also evaluated. In the case of aprotic solvents like toluene, CH_2Cl_2, THF, DMSO and acetonitrile (Figure 1 (a)), the reaction afforded unsatisfactory results comparing to protic solvents like EtOH, MeOH and water. Water could significantly enhance the yield of flavonols (Table 1, Entry 11). Interestingly, the formation of aurone was dominant (Table 1, Entry 10) in acetonitrile. It was noticeable that water was always necessary for mediation of the reaction, no products were detected without adding water, no matter what solvent was used other than water. Heating the reaction to 50 °C increased the yield of flavonol (Table 1, Entry 19 and 23, Figure 1, (b)), further elevation of the temperature from 50 °C to 80 °C decreased the yield of flavonol (Table 1, Entry 20-22, Figure 1, (b)). We noticed that air was necessary for the reaction. Accomplishing the reaction in the absence of oxygen, the reaction remained at the Claisen-Schmidt condensation step, neither flavonol nor aurone was detected except chalcone. On the other hand, the reaction under an oxygen-balloon instead of an aerobic condition gave increased total yields of flavonol and aurone. The careful exclusion of light completely suppressed the formation of product, confirming the photochemical nature of the process.

Table 1. Optimization of the Reaction Conditions [a]

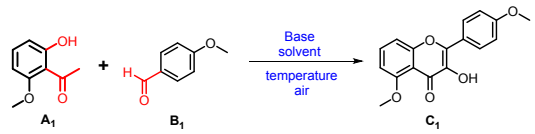

Entry	Base	Solvent	T(°C	Yield [b] (%)
1	n-propylamine	MeOH	rt	n. d
2	diethylamine	MeOH	rt	n. d
3	pyrrole	MeOH	rt	n. d.
4	piperidine	MeOH	rt	trace
5	pyrrolidine	MeOH	rt	40
6	L-proline	MeOH	rt	n. d
7	TBD	MeOH	rt	trace
8	Et_3N	MeOH	rt	n. d
9	pyrrolidine	EtOH	rt	35
10	pyrrolidine	CH_3CN	rt	8%(70%[d])
11	pyrrolidine	H_2O	rt	63%(29%[d])
12	pyrrolidine	THF	rt	11
13	pyrrolidine	DMSO	rt	15
14	pyrrolidine	Toluene	rt	trace
15	pyrrolidine	CH_2Cl_2	rt	trace
16	pyrrolidine	H_2O	20	50
17	pyrrolidine	H_2O	30	56
18	pyrrolidine	H_2O	40	61
19	**pyrrolidine**	**H_2O**	**50**	**73**
20	pyrrolidine	H_2O	60	65
21	pyrrolidine	H_2O	70	68
22	pyrrolidine	H_2O	80	70
23	pyrrolidine	H_2O	50	81[c]

[a] Reaction conditions: **A_1** (10 mg, 0.0602 mmol), **B_1** (7.7 μL, 0.0632 mmol), base (0.6020 mmol), and solvent 1.0 mL. The reaction was performed at the above temperature in air for 16 h. [b] Yield determined by HPLC analysis. [c] Reaction performed under an O_2 balloon. n.d = not detected. [d] Yields of aurone.

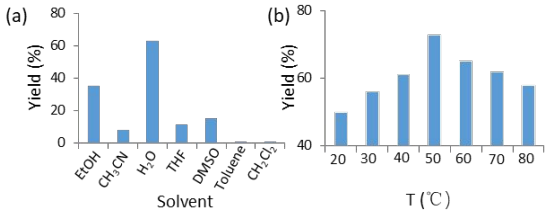

Figure 1. Schematic demonstration of the influence of reaction conditions on the model reaction: a) Solvents; b) Temperature.

Having identified an appropriate set of conditions, the optimized one-pot protocol was further extended to synthesis of different flavonol derivatives with/without 5-substituents, bearing both electrons donating and withdrawing groups (Table 2). Most 2'-hydroxylacetophenone without substituent at *C-6* were resulted in good yields, regardless of aldehyde types (Table 2, **C_{24}-C_{42}**). However, when 2'-hydroxylacetophenone (**A**) with substituent at *C-6* was subjected to the reaction, benzaldehydes (**B**) bearing electron withdrawing group (-Cl, -Br, -NO_2) afforded lower yields of flavonols (Table 2, **C_6-C_8**), and aurones were turned to be the major products. On the other hand, **B** bearing electron-donating groups (-OH, -OCH_3, -CH_3 and -$N(CH_3)_2$) were favorable for flavonol formation (Table 2, **C_1-C_4**, **C_9-C_{13}**, **C_{15}-C_{22}**). Particularly, All **B** with 4-hydroxyl group resulted in good yields (Table 2, **C_4**, **C_{19}**, **C_{28}**, **C_{37}**, **C_{39}**), regardless of the types of **A** used. **B** with 3-OH gave poorer yields than those with 4-OH (Table 2, **C_{10}**, **C_{20}**). In addition, **B** with 3-OCH_3, 4-OH or two functional groups gave lower yields than those with 4-OH only but gave higher yield than those with 4-OH and 3, 5-dimethoxyl ones (Table 2, **C_{11}**, **C_{13}**, **C_{22}**). We have also investigated **B** of aliphatic aldehydes, formaldehyde, propanaldehyde and valeraldehyde, but failed to obtain product. **A** with two electron-donating groups at *C-4* and *C-6* gave higher yield than those with single substituent at *C-6* (Table 2, **C_{17}-C_{23}**). Fluorine, instead of methoxy group at *C-6* of **A** did not affect the yields of flavonol significantly (Table 2, **C_{15}-C_{16}**). Although **A** with substituent at *C-4* or *C-5* gave higher yields than those with functional group at *C-6*, but still afforded poorer yields than those of unsubstituted **A** (Table 2, **C_{35}-C_{42}**). When thiophenone was subjected for the reaction, the presence or absence of *C-6* on A had little effect on the yields (Table 2, **C_{14}**, **C_{34}**). Comparing with the AFO reaction, the yields of flavonol based on this protocol were enhanced about 20%-40%.

The efficiency of this method on a larger scale was next investigated. It is noteworthy that this procedure can be scaled up to gram quantities of the desired flavonols and aurones without sacrificing yields. For example, 3.339 g of C_1 and 4.293 g of D_8 could be isolated in 62% and 80% yields respectively, highlighting the synthetic utility of this method.

To elaborate the synthetic utility further, we then adapt the method for natural flavonols synthesis. Three natural flavonols: isorhamnetin, tamarixrtin, and kaempferide were successfully synthesized in three steps: selective protection of acetophenol, formation of flavonol and deprotection, with successive yields of 41%, 64% and 65%, (Scheme 2), corresponding to 15% (six steps), 15% (six steps) and 25% (five steps) as reported with protection-deprotection processes.[20]

We then focused on the mechanism. The aerobic oxidation without additional oxidant in which this reaction proceeds suggested a distinct mechanism compared to previously reported hydrogen peroxide procedures (AFO reaction).

We started with tracking the oxygen source of 3-OH in flavonol. First, isotope oxygen $^{18}O_2$ gas in balloon was used instead of air for the model reaction. The products flavonol (69%) and aurone (22%) were analyzed by high-resolution mass spectroscopy (HR-ESI-MS), in which ^{18}O containing flavonol was detected, but no ^{18}O labelled aurone was found (Scheme 3 (a) and Figure S1). Next, $H_2{}^{18}O$ was used as solvent in the model reaction. Indeed, both ^{18}O contained flavonol (61%) and aurone (28%) (Scheme 3 (b), Figure S2) were obtained. Furthermore, $H_2{}^{18}O$ and $^{18}O_2$ gas balloon were used together for the model reaction, two ^{18}O isotopes containing $(^{18}O)_2$-C_1 (70%) and only one isotope containing ^{18}O-D_1 (20%) were isolated (Scheme 3 (c), Figure S3). The above isotope tracking experiments together revealed that oxygen atom at C-3 of flavonol came from atmospheric oxygen in the environment and the oxygen atom of the carbonyl in both flavonol and aurone were from water.

Next, we turned to investigate the key intermediate(s) leading to flavonol and aurone. We conducted *in-situ* ^1H NMR monitor for the model reaction. After 10 mins of the reaction, we found a proton signal appeared at δ 7.33, which could be assigned to Hd (Figure S4), the typical indicator of β-proton of α, β-unsaturated imine. Prolonging the reaction to 30 mins, the signal at δ7.33 was increased, showing that almost all starting materials converted into this intermediate (Figure S4). This intermediate is quite stable under the oxygen deficient condition in a capped NMR tube. It took several hours before the intermediate changed. Thus, we were able to do HMBC (Figure S8) and HSQC (Figure S7) experiments to determine the structure of the intermediate. An α-

deuterated eniminium ion (Since CD_3OD and D_2O were used), could be assigned to the intermediate as $\mathbf{E_1}$ (Figure S4). During the transformation from $\mathbf{E_1}$ to $\mathbf{C_1}$ and $\mathbf{D_1}$, a number of intermediates were emerged which were unable to be identified from *in-situ* ^{1}H NMR measurement (Figure S5-6).

Being established that the eniminium $\mathbf{E_1}$ was the key intermediate leading to flavonol and aurone, we next tried to explore the origin in directing the selectivity from $\mathbf{E_1}$ to flavonol and aurone. The first question arises to whether flavonol and aurone generated through the same pathway or different pathways. We found that the formation of aurone ($\mathbf{D_1}$) was ceased by the addition of 2, 2, 6, 6-tetramethylpiperidine 1-oxyl (TEMPO, 2 equivalents) into the model reaction, in the meantime, the generation of flavonol was not affected. This is indicative of a radical mechanism for the formation of aurone and a non-radical mechanism for the generation of flavonol. In other words, two different pathways were involved in the reaction. To further confirm that TEMPO inhibits the generation of aurone, we added TEMPO to the reaction of $\mathbf{A_1}$, and $\mathbf{B_6}$, and $\mathbf{A_1}$ and $\mathbf{B_7}$, also found that aurones ($\mathbf{D_6}$ and $\mathbf{D_7}$) were also inhibited, in the meantime, the yields of $\mathbf{C_6}$ and $\mathbf{C_7}$ were remained unaffected. Thus, we could

Table 2. Synthesis of Flavonols

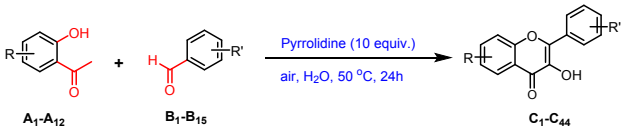

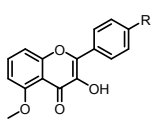

C1: R=OCH_3, 63% (29%)[c]
C2: R=$N(CH_3)_2$, 85%
C3: R=CH_3, 60% (28%)[c]
C4: R=OH, 85%
C5: R=H, 35% (52%)[c]
C6: R=Cl, 10% (72%)[c]
C7: R=Br, trace (75%)[c]
C8: R=NO_2, trace (81%)[c]

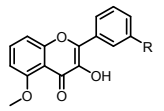

C9: R=CH_3, 42% (47%)[c]
C10:R=OH, 52% (44%)[b]

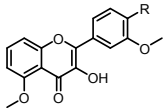

C11: R=OH, 83%
C12: R=OCH_3, 61% (31%)[c]

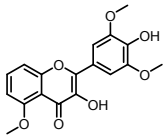

C13: 50% (30%)[c]

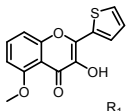

C14: 76%

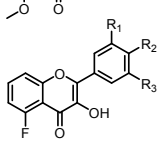

C15: R_1=R_3=H, R_2=OCH_3, 81%
C16: R_1=R_2=R_3=OCH_3, 78%

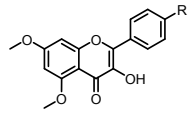

C17: R=OCH_3, 85%
C18: R=$N(CH_3)_2$, 90%
C19: R=OH, 82%

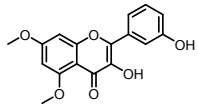

C20: 68% (19%)[c]

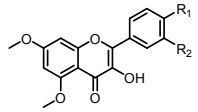

C21: R_1=R_2=OCH_3, 85%
C22: R_1=OH,R_2=OCH_3, 80%

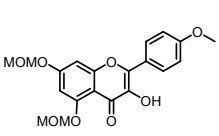

C23: 88%

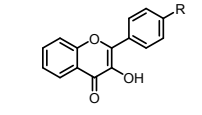

C24: R=H, 78%
C25: R=CH_3, 80%
C26: R=$N(CH_3)_2$, 87%
C27: R=OCH_3, 89%
C28: R=OH, 86%
C29: R=Cl, 85%
C30: R=Br, 80%

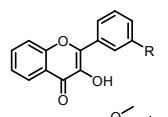

C31: R=OCH_3, 70%
C32: R=OH, 91%

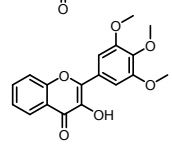

C33: 74%

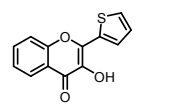

C34: 75%

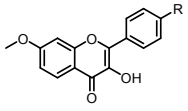

C35: R=H, 72%
C36: R=OCH_3, 76%
C37: R=OH, 85%

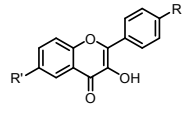

C38: R'=OCH_3, R=H, 75%
C39: R'=OCH_3, R=OH, 81%
C40: R'=F, R=H, 78%
C41: R'=Cl, R=H, 81%
C42: R'=Br, R=H, 82%
C43: R'=NO_2, R=$N(C_2H_5)_2$, 38%
C44: R'=Br, R=$N(C_2H_5)_2$, 45%

[a] Reaction conditions: Reactions were carried out with A (1.2 mmol, 1.0 equiv.), B (1.26 mmol , 1.05 equiv.),H_2O 20 mL, and pyrrolidine (12 mmol, 10 equiv.) at 50 °C in air for 24 h.
[b] Isolated yield of purified material.
[c] Aurone yields.

Scheme 2. Convenient Synthesis of Natural Products

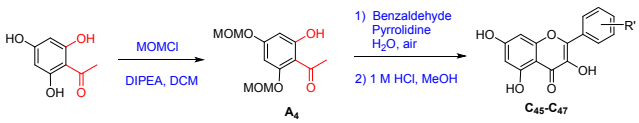

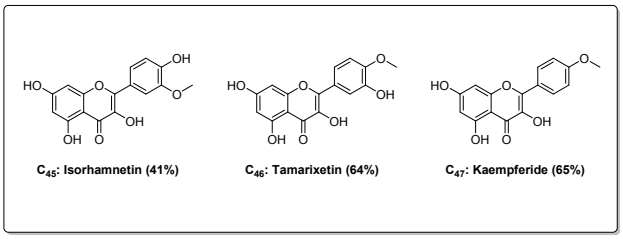

Scheme 3. $H_2{}^{18}O$ and $^{18}O_2$ Tracking for the Model Reaction

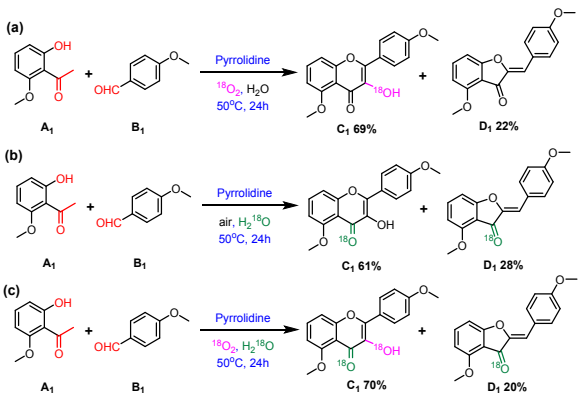

conclude that different pathways are involved in formation of flavonol or aurone. Since both flavonol and aurone were generated in the model reaction, it is impossible to differentiate intermediates of one path (for flavonol) from the other (for aurone) within the same reaction. Fortunately, during the preparation of $\mathbf{C_4}$ from $\mathbf{A_1}$ and $\mathbf{B_4}$ in water, we noticed some precipitates generated when the first drops of pyrrolidines were added into the aqueous solution of $\mathbf{A_1}$ and $\mathbf{B_4}$. The precipitate was isolated and characterized by ^{1}H NMR, ^{13}C NMR, HSQC, HMBC, HR-ESI-MS and elementary analysis. The data together indicate that this precipitate is an aggregate of $\mathbf{E_4}$, with a formula of $\mathbf{2E_4.H_2O}$ (Figure S9-12) Addition of 9 equivalents of pyrrolidine into the mixture of the isolated solids in water, flavonol $\mathbf{C_4}$ was generated almost quantitatively, no aurones were detected in this reaction (Scheme 4 (a)).

In addition, during the reaction of $\mathbf{A_1}$ and $\mathbf{B_{13}}$ in acetonitrile, we noticed some purple solid precipitated out from the solution when 4 equivalents of pyrrolidines were added. Further addition of pyrrolidine into the suspension of the purple solids in water, methanol or acetonitrile respectively, resulted in no product. Neutralization of the purple solids with 3N of HCl solution, a yellow powder was obtained by extraction with dichloromethane. The structure of the yellow powder was proved to be the enimine salt $\mathbf{2E_{13}HCl.H_2O}$ from ^{1}H NMR, ^{13}C NMR, HR-ESI-MS (Figure S15-16), element analysis and single X-ray crystallographic analysis together. (Figure S17). Surprisingly, addition of 9 equivalents of pyrrolidines into the solution of $\mathbf{E_{13}HCl}$ in acetonitrile, only aurone was obtained.

With the two isolated enamine aggregate intermediates $\mathbf{E_4}$ and $\mathbf{E_{13}HCl}$ in hand, now we are able to investigate the path leading to flavonol or aurone respectively. Two possible trajectories to flavonol from $\mathbf{E_4}$ are assumed. One is the cyclization followed oxidation and the other is the epoxidation-cyclization. (Scheme 5 (a) and (b)). To investigate the trajectory to flavonol, we conducted the reactions of $\mathbf{E_4}$ catalysed by 9 equivalents of pyrrolidine in water, methanol and acetonitrile, respectively, as presented in Scheme 4, (a), (b) and (c). We found that flavonol $\mathbf{C_4}$ was generated with 80% yield in water (Scheme 4, (a)), 40% yield in methanol (scheme 4, (b)), and trace $\mathbf{C_4}$ in acetonitrile (Scheme 4, (c)). Addition of TEMPO into the above reactions had no effect on the yields of $\mathbf{C_4}$, indicating that the generation of flavonol is not a radical mechanism.

However, addition of H_2O_2 into the suspension of $\mathbf{E_4}$ in water, dihydrogenflavonol ($\mathbf{V_4}$) was obtained with 85% yield (Scheme 4, (d)), which is known through an epoxide intermediate path[21]. Thus, the epoxide path (Scheme 5(b)) could be excluded from $\mathbf{E_4}$ to $\mathbf{C_4}$ by pyrrolidine catalysis. We speculated that the cyclization-oxidation process is accounted for the trajectory from $\mathbf{E}$ to $\mathbf{C}$ by pyrrolidine catalysis.

Scheme 4. Reactions of $\mathbf{E_4}$ with pyrrolidine catalysis in different solvents: a) H_2O, b) CH_3OH, c) CH_3CN, and (d) with H_2O_2

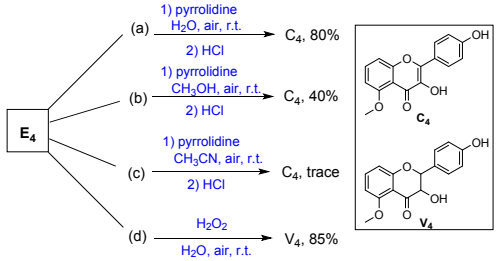

Scheme 5. Possible trajectories' from $\mathbf{E_4}$ to $\mathbf{C_4}$: a) cyclization-oxidation; b) oxidation-cyclization

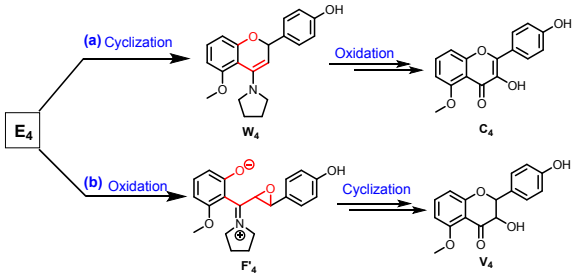

Next, we investigate the pathway from $\mathbf{E_{13}}$ to aurone by the following experiments: 1) The reaction of $\mathbf{A_1}$ and $\mathbf{B_{13}}$ (one-pot reaction) under 9 equivalents of pyrrolidine in water produced 50% $\mathbf{C_{13}}$ and 30% $\mathbf{D_{13}}$. (Scheme 6, (a)); 2) On the other hand, the reaction of $\mathbf{E_{13}HCl}$ under the same condition did not give either $\mathbf{C_{13}}$ or $\mathbf{D_{13}}$. (Scheme 6, (d)); 3) By switch the solvent to acetonitrile, the reaction of Scheme 6 (a) and (d) under the otherwise identical conditions, afforded $\mathbf{D_{13}}$ only with yield of 20% and 30%, respectively (Scheme 6, (b) and (e)); 4) Addition of TEMPO into the reactions of Scheme 6 (a), (b) and (e) inhibited the formation of $\mathbf{D_{13}}$; 5) Both the one-pot reaction and the reaction of $\mathbf{E_{13}HCl}$ in water with $NaOH/H_2O_2$ resulted in dihydrogen flavonol $\mathbf{V_{13}}$ only, with yields of 85% and 80% respectively. (Scheme 6, (c) and (f)) Interestingly, $\mathbf{V_{13}}$ could not be converted into $\mathbf{C_{13}}$ by addition of pyrrolidines or H_2O_2.

Scheme 6. Reactivity of iminium ion $\mathbf{E_{13}}$.HCl; $\mathbf{A_1}$ and $\mathbf{B_{13}}$.

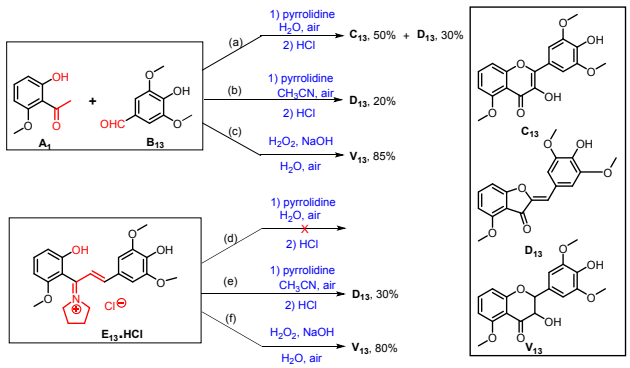

The above reactions demonstrate that the formation of both flavonol and aurone in the presence of pyrrolidine is not from the epoxide intermediate. A radical mechanism for the formation of aurone can be confirmed. The selectivity of flavonol or aurone is solvent dependent for a same substrate.

After knowing that the reaction pathways leading to flavonol and aurone are heavily solvent dependent, it is necessary to identify the intermediates involved in different solvents. The advantage of UV-vis spectra lies in the fact that it can differentiate between the multitude of reaction species. Thus, we turned to investigate the solvent triggered formats of $\mathbf{E_4}$ and $\mathbf{E_{13}HCl}$ by UV-vis spectra. UV-vis absorption spectra of $\mathbf{E_4}$ (red), $\mathbf{E_4}$ with equal molar HCl (break line) and $\mathbf{E_4}$ in the presence of 0-10 equivalents of pyrrolidine (plain lines) in water and acetonitrile were recorded respectively, as presented in Figure 2 (2) and (3). It is clear that the bands at 378 nm in water, and 380 nm in acetonitrile of $\mathbf{E_4}$ were overlapped with those of $\mathbf{E_4HCl}$ in corresponding solvents, which was assigned to the enol-imine intermediate $\mathbf{E_4}$-$\mathbf{A}$ (Figure 2 (1)). The structure of $\mathbf{E_4HCl}$ was confirmed by ^{1}H NMR and ^{13}C NMR (Figure S13-14). In addition, during electrospray mass spectrometry (ESI_MS) spectra for *in-*

situ analysis of the model reaction, the mass peaks at m/z 338.1759 and 356.1758 corresponding to $\mathbf{E_1}$ and $\mathbf{E_1H_2O}$ are clearly observed (Figure S24), which give solid evidence for the formation of $\mathbf{E_1H_2O}$.

The UV-vis spectrum of $\mathbf{E_4}$ in water with the gradual addition of pyrrolidine is characterised by a new band centered at 448 nm, at the same time the absorption at 378 nm ($\mathbf{E_4}$**-A**) decreased sharply with no isosbestic point. (Figure 2, (2)). Such a phenomenal implies that the band at 448 nm in water correspond to a species which is not an isomer of $\mathbf{E_4}$**-A**, but a new species. According to the linear Benesi-Hildebrand expression[22], the measured absorbance $[1/(A\text{-}A_0)]$ at 448 nm varied as a function of 1/[pyrrolidine] in a linear relationship (R=0.9955) (Figure S22, (2)), indicating the 1 : 1 stoichiometry bewtween the pyrrolidine and $\mathbf{E_4}$ with the associate constant of 9.06 x 10^3 M^{-1}. On the basis of UV-vis data in Figure 2 (2) and the fact that the reaction of $\mathbf{E_4}$ in water in the presence of pyrrolidine produces flavonol $\mathbf{C_4}$ only, the band at 448 nm could be attributed to a solvated $\mathbf{E_4}$**-I,** which could be cyclized to $\mathbf{F_4}$ and oxadized to $\mathbf{G_4}$ under the presence of singlet oxygen through an electron transfer process[23]. Successive ring open of $\mathbf{G_4}$ and hydrolysis afforded flavonol.

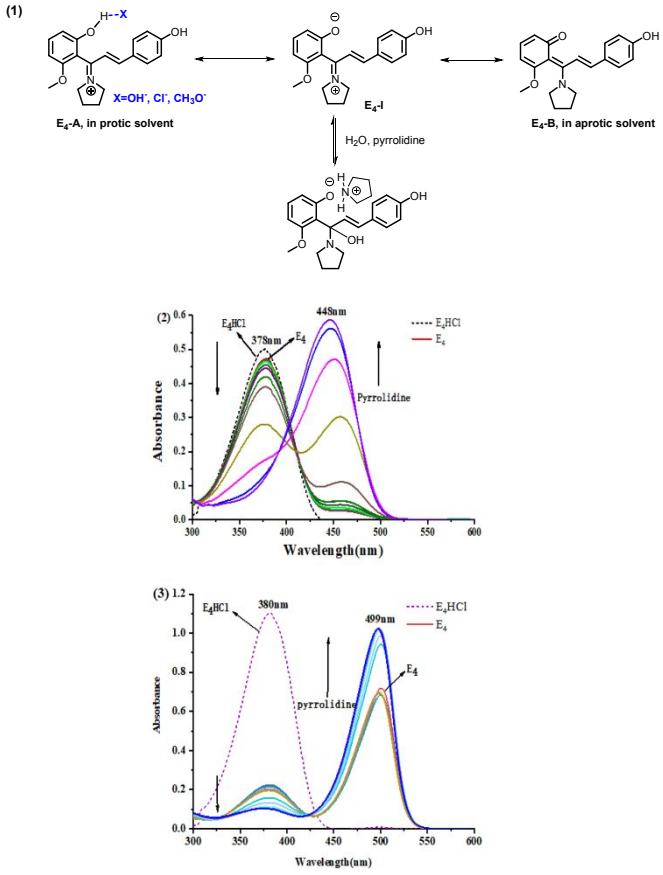

Figure 2 (1) The predicted formats of $\mathbf{E_4}$ from UV-visible spectra. (2) UV-vis absorption spectra of $\mathbf{E_4}$ (1.7×10^{-5} M), $\mathbf{E_4}$ plus 1eq of HCl and $\mathbf{E_4}$ plus 0-10 eq. pyrrolidine in water and (3) in acetonitrile

On the other hand, the very intense band of $\mathbf{E_4}$ in acetonitrile at 499 nm arises as the increasing concentration of pyrrolidine, at the same time the absorption at 380 nm ($\mathbf{E_4}$**-A**) decreased sharply with an isosbestic point at 423 nm. (Figure 2 (3)), indicating that the band at 499 nm and $\mathbf{E_4}$**-A** are two inter-changable isomers. The measured absorbance $[1/(A–A_0)]$ at 499 nm varied as a function of 1/[pyrrolidine]^2 (R=0.9953) according to the linear Benesi–Hildebrand expression, suggesting the 1 : 2 stoichiometry between the pyrrolidine and $\mathbf{E_4}$**-B** with an association constant of 7.92 x 10^3 M^{-1} (Figure S22, (4)). Based on the UV-vis data, the band at 499 nm could be assigned to $\mathbf{E_4}$**-B**. Due to $\mathbf{E_4}$ is not soluble in acetonitrile, $\mathbf{E_4}$**-B** cannot be characterized by spectroscopy methods.

To understand the pathway involved in the formation of aurone, the UV-vis spetra of $\mathbf{E_{13}HCl}$ (break line) and $\mathbf{E_{13}HCl}$ with an increasing pyrrolidine amount from 0.2 to 10 equivalents in water (Figure 3, (2))and acetonitrile (Figure 3, (3)) were recorded and analyzed. The absorption spectra of $\mathbf{E_{13}HCl}$ mesured in water exhibit one band at 408 nm (Figure 3, (2)), which could be assigned to $\mathbf{E_{13}}$**-A**. The structure of $\mathbf{E_{13}}$**-A** was confirmed by ^{1}H NMR and ^{13}C NMR. (Figure S15-16) from $\mathbf{E_{13}HCl}$ and crstal strucutre (Figure S17)

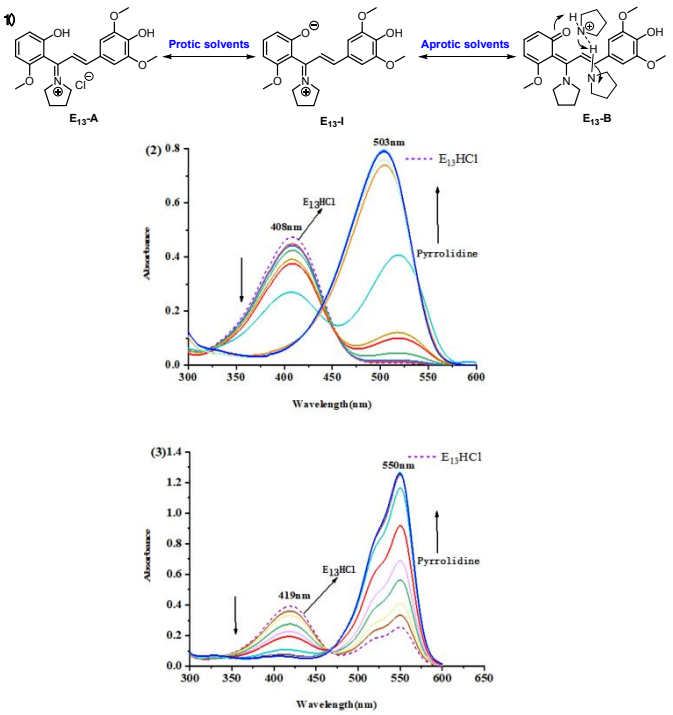

Figure 3 (1) The predicted formats of $\mathbf{E_{13}}$ from UV-visible spectra. (2) UV-vis absorption spectra of $\mathbf{E_{13}}$HCl (1.7×10^{-5} M) and $\mathbf{E_{13}}$ plus 0-10 eq. pyrrolidine in water and (3) in acetonitrile.

However, the absorption spectrum of $\mathbf{E_{13}HCl}$ in acetonitrile shows two bands at 419 nm and 550 nm (Figure 3, (3)). Further addition of pyrrolidine into solution of $\mathbf{E_{13}HCl}$ in acetonitrile did not shift the two bands but leads to a continuous decrease in the 419 nm of the $\mathbf{E_{13}}$**-A** band, along with an increase in the 550 nm band with an isosbestic point existed at 467nm. The measured absorbance $[1/(A\text{-}A_0)$ at 550 in acetonitrile give a linear relationship with a change of 1/[pyrrolidine]^2 (R=0.999), indicating a 1 : 2 stoichiometry between pyrrolidine and $\mathbf{E_{13}HCl}$, with the associate constant of 1.46 x 10^4 M^{-1}. (Figure S23, (4)). On the basis of UV-vis data in Figure 3 (3) and the fact that the reaction of $\mathbf{E_{13}}$ in acetonitrile in the presence of pyrrolidine generates aurone $\mathbf{D_{13}}$ only, the band at 550 nm was assigned to $\mathbf{E_{13}}$**-B**, which was associated with two molar of pyrrolidine. (Figure 3 (1)). On the other hand, addition of pyrrolidine in water shifted the band at 408 nm to a prevalent new band at 503 nm, but no isosbestic point was observed (Figure 3, (2)) indicating that this species is not a tautomer of either $\mathbf{E_{13}}$**-A** or $\mathbf{E_{13}}$**-B**. According to the linear Benesi-Hidebrand expression, the measured

absorbance [1/(A-A_0)] in water at 503 shows a linear relashioship with a change of 1/[pyrrolidine] (R=0.9953), indicating a 1 : 1 stoichiometry between pyrrolidine and **E_{13}HCl** (Figure S23, (2)) with the association constant of 1.69 x 10^3 M^{-1}.

On the basis of our preliminary experimental observations that the format of intermediates depended on the solvent, and the product selectivity as well, we anticipate that the solvent triggled intermediate formats of enolimine (**E-A**) and ketoenamine (**E-B**) determine the products selectivity.

1） In protic solvents, e.g. in water, **E-A** is dominant, which is tend to form the zwitterionic-like intermediate (**E-I**) under the presence of pyrrolidine, followed by cyclization to afford **F**, [2+2] oxidation of **F** with singlet oxygen leading to flavonol. (Scheme 7, a).

2） On the other hand, in aprotic solvent (e.g. acetonitrile) **E-B** is prevalent, generating enamine **K** through the Michael reaction with pyrrolidine., The radical pair of **L** and hydrogenperoxide (Scheme 8 b) were initialized in the presence of pyrrolidine and O_2 under visible light. Successive radical oxidation, cyclization, depyrrolidine and hydrolysis affored aurone (Scheme 7, b).

Scheme 7. Intermediates involved in the transformations from (a) E-A to Flavonol and (b) E-B to Aurone

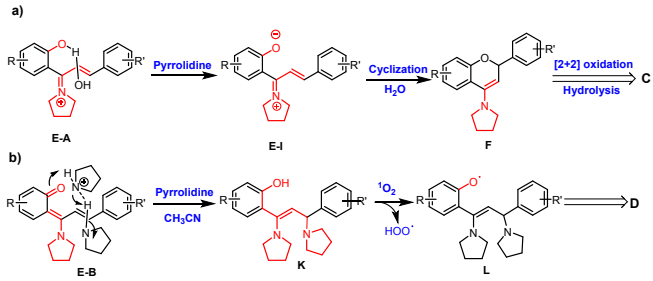

The generation of phenoxyl radical under the presence of O_2 and light was proposed by Novak et al.[24]. Thus, we can undertand the phenominas: 1). **E_4** does not react in acetonitrile and only produces flavonol in water, since there is no **E_4-B** existed in the reaction system. (Scheme 4, (c)) 2). **E_{13}HCl** generates aurone only in acetonitrile, because **E_{13}-B** is existed as the only intermediate specie. However, we could not understand why the one-pot reaction could produce flavonol **C_{13}** but not from **E_{13}** or **E_{13}HCl**.

Scheme 8. Proposed mechanism

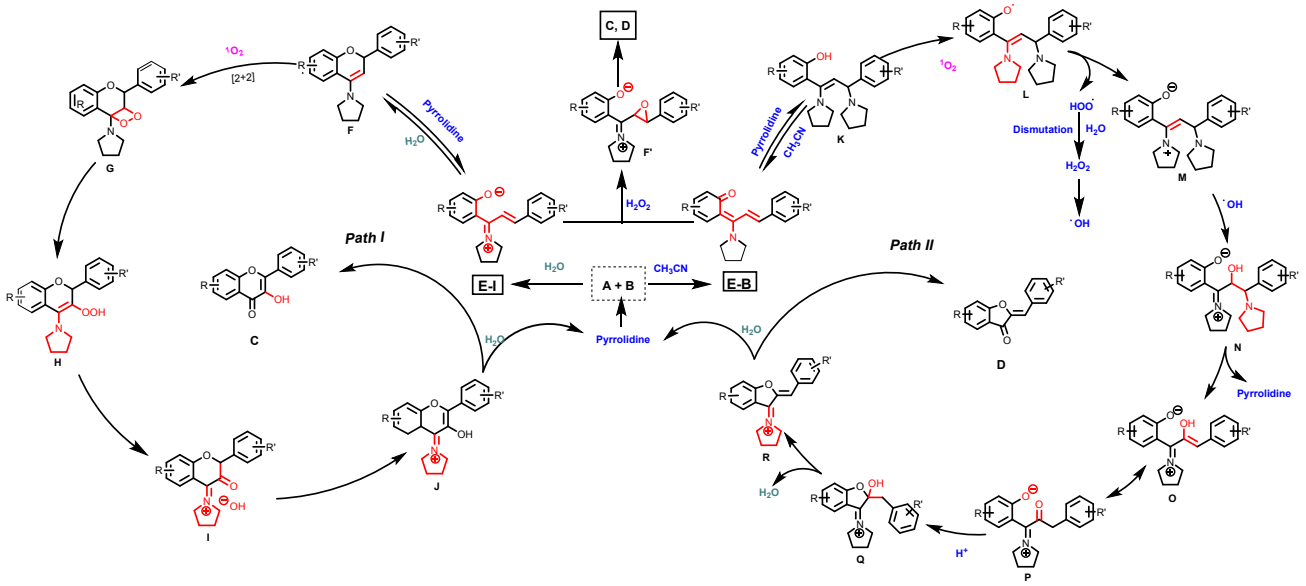

A plausible two-pathway reaction mechanism for the formation of flavonol and aurone can be proposed, as illustrated in Scheme 8. The reaction in protic solvent, i.e. water, takes place through path I that begins with the cyclization of the zwitterionic phenoxy-iminium ion **E-I**, which was generated from **E-A** in the presence of pyrrolidine, to afford **F**, successive [2+2] oxidation of the cyclic enamine **F** by $^1O_2$ form dioxetane **G**. Ring opening of **G** gave peroxide intermediate **H**, rearrangement of **H** through **I** to **J**, followed by hydrolysis finished flavonol **C**. The proposed intermediates in Path I were identified by a set of LC-ESI-MS experiments for the reaction of **E_4** in water proceeds in under 40 min (Scheme 4 (a), Figure S25). The intramolecular Michael product **F_4** was detected at *m/z* 324.1606 with a retention time of 1.792 min which can be differentiate from **E_4-A** (*m/z* 324.1652, retention time 1.576 min). At this time point, there is no detectable *m/z* signals belong to **G_4** was observed, probably due to its very short lifetime. However, *m/z* signals that correlate to peroxide intermediate **H_4** (ring opening of **G_4**) and **I_4** (rearrangement of **H**) was detected as $[\mathbf{H_4}+H]^+$ at *m/z* 356.1407. *m/z* 338.1440 could be assigned to $[\mathbf{I_4}]^+$ and its taotomeric form **J_4**. The final produc **C_4** was conformed by *m/z* 285.0745.

On the other hand, the reaction in aprotic solvent, i.e. acetonitrile, takes place through Path II that starts from the Michael reaction between **E-B** and pyrrolidine, and concomitant generation of the radical pair precursors of **L** and HOO· to adducts **M** arising by intramolecular electron transfer. HOO· would conversion into H_2O_2 by dismutation under the presence of water, the precursor of highly reactive OH·[25]. Photoaddition of **M** and

HO· to afford **N**. Retro-Michael reaction of **N** resulted in **O**. Tautomerization of **O** generates **P**, which proceeds through cylization and dehydration to resulted in **R**. Aurone was finalized by hydration of the iminium precursor **R**. The proposed intermediates in Path II were identified by a set of LC-ESI-MS experiments of $\mathbf{E_{13}HCl}$ in acetonitrile (Scheme 6 (e)), Figure S26). *m/z* 455.2200 ($[\mathbf{K_{13}}+H]^+$) was detected, which could be assigned to the Michael product of **E-B**. Although the radical species $\mathbf{L_{13}}$ and $\mathbf{M_{13}}$ could not be detected, the adduct $\mathbf{N_{13}}$ of $\mathbf{M_{13}}$ and the hydroxyl radical was recognized ($[\mathbf{N_{13}}+Na]^+$ *m/z* 493.3276). The intermediate $\mathbf{O_{13}}$ resulted by the elimination of pyrrolidine from $\mathbf{N_{13}}$, as well as its tautomeric format $\mathbf{P_{13}}$ and successive cyclization intermediate $\mathbf{Q_{13}}$, were detected at *m/z* 400.2017). $\mathbf{R_{13}}$ (not detectable from LCMS) could be generated from dehydration of $\mathbf{Q_{13}}$ and simultaneously hydrolyzed to $\mathbf{D_{13}}$. The final product $\mathbf{D_{13}}$ was confirmed by the fragment at *m/z* 329.1019, of $[\mathbf{D_{13}}+H]^+$.

It should be pointed out that for most substrates, both flavonol and aurone were produced, since both **E-A** and **E-B** were existed in either water or acetonitrile. The effects of different lifetime of singlet oxygen in water and acetonitrile to the product selectivity also could not be excluded. Since the lifetime of singlet oxygen in water (3.1 μs) is much shorter than in acetonitrile (77.1 μs).[26] The activation energy of [2+2] oxidation in Path I might be higher than that of the radical reaction in Path II. Therefore, typically, higher reaction temperature is favored in preparation of flavonols. The minor existence of epoxide, which leads to both flavonol and aurone cannot be excluded, since dihydrogenflavonol was detected from the model reaction. Density functional theory (DFT) calculations for the cyclization of epoxide intermediate ($\mathbf{G'_1}$). The results suggest that the barrier is higher for flavonol $\mathbf{C_1}$ formation than that of aurone $\mathbf{D_1}$. (Figure S27). If flavonol and aurone are developed mainly from the epoxide, aurone $\mathbf{D_1}$ should be obtained as the major product rather than flavonol $\mathbf{C_1}$. This was in controversial to our experimental observations. Thus, the proposed mechanism of path I for flavonol and path II for aurone was plausible.

At current state, although we are not sure of which species works as the sensitizer to promote the reactive oxygen species (ROS), but both the enamine **E** and pyrrolidine are responsible for the generation of ROS, since no oxidation of **E** was observed in the absence pyrrolidine or pyrrolidine was oxidized without **E**. The requirements for light and 10 equivalents of pyrrolidine in effecting the reaction are indicative of photochemical nature of the reaction and the function of pyrrolidine in initiation of ROS.

Based on the mechanism, we could understand the influence of both the steric and electronic property of substrates on the selectivity of products. All substrates without a 5-substituent are favorable in producing flavonols through cyclizarion of the zwitterionic-like intermediate **E-I**, due to the easy formation of **E-A** and co-planar effect of the phenoxide of A-ring with imine ion (Table 2, $\mathbf{C_{24}}$-$\mathbf{C_{42}}$). In addition, substrates with electron donation group(s), such as those of -OH, $-OCH_3$, $-CH_3$, and $-N(CH_3)_2$ on B-ring, would stabilize the formation of **E-A**, which proceeded favorably to generate the zwitterionic phenoxy-iminium intermediate **E-I** in the presence of pyrrolidine, following path I to afford flavonols (Table 2, $\mathbf{C_1}$-$\mathbf{C_4}$, $\mathbf{C_9}$-$\mathbf{C_{13}}$, $\mathbf{C_{15}}$-$\mathbf{C_{23}}$, $\mathbf{C_{25}}$-$\mathbf{C_{28}}$, $\mathbf{C_{31}}$-$\mathbf{C_{33}}$, $\mathbf{C_{36}}$-$\mathbf{C_{37}}$, $\mathbf{C_{39}}$). Substrates with –OH group at *C′–4* of B-ring gave excellent yields (Table 2, $\mathbf{C_4}$ (85%), $\mathbf{C_{19}}$ (82%), $\mathbf{C_{28}}$ (86%), $\mathbf{C_{37}}$ (85%), $\mathbf{C_{39}}$ (81%), regardless of the types of substituents on A-ring. Whereas the substrates with 5-substituent on A-ring and/or electron-withdrawing groups on B-ring, such as –Cl, -Br and $-NO_2$, would favor the formation of **E-B**, which would successively going through path II to produce aurones (Table 2, $\mathbf{C_6}$-$\mathbf{C_8}$). The stereoscopic effect is greater than the electronic effect in the reaction. **A**-ring without substituent at *C-5* were resulted in good yields, regardless of the substituent of B-ring (Table 2, $\mathbf{C_{24}}$-$\mathbf{C_{42}}$). **A**-ring with a group at *C-5* and **B**-ring with electron withdrawing group (-Cl, -Br, $-NO_2$) afforded lower yields of flavonols, and aurones were turned to be the major products. (Table 2, $\mathbf{D_6}$ (72%), $\mathbf{D_7}$ (75%), and $\mathbf{D_8}$ (81%)).

■ CONCLUSION

In summary, we have developed a one-pot aerobic oxidative synthesis of flavonols from 2′-hydroxyl-acetophenone and benzaldehyde in the presence of pyrrolidine in water under atmospheric condition.

Our preliminary mechanistic investigation demonstrates that the selectivity for flavonol or aurone was originated from solvent triggered intermediates, the phenol-iminium **E-A** and the ketoenamine intermediate **E-B**. Consequently, formation of flavonol was favored in the presence of pyrrolidine in water through cyclization of the zwitterionic phenoxy-iminium ion **E-I** followed by [2+2] reaction with $^1O_2$, whereas the Michael reaction between in-situ generated **E-A** and pyrrolidyl anion, followed by a radical oxidation in the presence of pyrrolidine in aprotic solvent, was accounted for the pathway leading to aurone. Our results should provide valuable information not only for optimization of synthetic methods for flavonols, but also for the design of new amine catalyzed ROS reactions. Further studies are underway in our group to elucidate the fundamental ROS generations and the theoretical investigation of the reactivates of solvent dependent intermediates toward the cyclization/ [2+2] oxidation and the Michael /radical processes.

■ EXPERIMENTAL PART

General Information. All commercially available chemicals and reagents were used without any further purification unless mentioned otherwise. Melting Points were determined by X-6 apparatus without correction. Chromatographic purification was performed on silica gel (200-300 mesh). Analytical thin layer chromatography (TLC) was performed on silica gel 60-F_{254} (Qindao, China), which was detected by fluorescence. ^{1}H NMR spectra were recorded on 400 MHz, 600 MHz and 800 MHz. ^{13}C NMR spectra were recorded at 101, 151 or 201 MHz. Assignments of ^{1}H NMR and ^{13}C NMR signals were made, where possible, using HSQC and HMBC experiments. The spectra were recorded in $CDCl_3$, DMSO-d_6, CD_3OD, or Acetone-d_6 as the solvent. The peaks around δ 7.26 (^{1}H NMR) and 77.16 (^{13}C NMR) correspond to $CDCl_3$. The peaks around δ 2.50 (^{1}H NMR) and 39.52 (^{13}C NMR) correspond to DMSO-d_6. The peaks around δ 3.31 (^{1}H NMR) and 49.01 (^{13}C NMR) correspond to CD_3OD. The peaks around δ 2.05 (^{1}H NMR), 29.84 (^{13}C NMR) and 206.26 (^{13}C NMR) correspond to Acetone-d_6. Multiplicities are indicated as follows: s (singlet), d (doublet), t (triplet), dd (doublet of doublets), etc. Coupling constants (J) are given in hertz. Chemical shifts (δ) are reported in parts per million relative to TMS as an internal standard. The ESI-HRMS was carried out on a Bruker Bio TOF IIIQ (quadrupole time of flight) mass spectrometer.

General Procedure for the Preparation of Flavonols. Pyrrolidine (12.04 mmol, 10.0 equiv.) was added to a suspending solution of acetophenone **A** (1.204 mmol, 1.0 equiv.), benzaldehyde **B** (1.26 mmol, 1.05 equiv.) in H_2O (20 mL) under an atmospheric condition. The resulting mixture was stirred at 50 °C (oil bath) for 24 h then cooled to room temperature. The mixture was poured into ice-cold water and acidified with HCl aqueous solution (30%, v/v) to pH=4. The produced precipitate was filtered and washed with water and ethanol. The crude

products were recrystallized from ethanol to afford flavonol **C**. All products were similarly purified by crystallization, except $\mathbf{C_1}$, $\mathbf{C_3}$, $\mathbf{C_5}$-$\mathbf{C_{10}}$, $\mathbf{C_{12}}$-$\mathbf{C_{13}}$, and $\mathbf{C_{20}}$, which were obtained by flash silica gel column chromatography (PE/EA), since aurone ($\mathbf{D_1}$, $\mathbf{D_3}$, $\mathbf{D_5}$-$\mathbf{D_{10}}$, $\mathbf{D_{12}}$ -$\mathbf{D_{13}}$, $\mathbf{D_{20}}$) was produced.

A Gram Scale Synthesis of $\mathbf{C_1}$: Pyrrolidine (14.817 mL, 10.0 equiv.) was added to a suspending solution of acetophenone $\mathbf{A_1}$ (3.000 g, 1.0 equiv.), benzaldehyde $\mathbf{B_1}$ (2.701 g, 1.1 equiv.) in H_2O (120 mL) and CH_3OH (10 mL) under an atmospheric condition. The resulting mixture was stirred at 50 °C (oil bath) for 24 h then cooled to room temperature. The mixture was poured into ice-cold water and acidified with HCl aqueous solution (30%, v/v) to pH=4. The purification process followed the general procedure. The isolated products $\mathbf{C_1}$ (3.339 g, 62%) were obtained.

A Gram Scale Synthesis of $\mathbf{D_8}$: Pyrrolidine (14.817 mL, 10.0 equiv.) was added to a suspending solution of acetophenone $\mathbf{A_1}$ (3.000 g, 1.0 equiv.), benzaldehyde $\mathbf{B_8}$ (3.001 g, 1.1 equiv.) in CH_3CN (120 mL) and H_2O (10 mL) under an atmospheric condition. The resulting mixture was stirred at 50 °C (oil bath) for 24 h then cooled to room temperature. The mixture was poured into ice-cold water and acidified with HCl aqueous solution (30%, v/v) to pH=4. The purification process followed the general procedure. The isolated products $\mathbf{D_8}$ (4.293 g, 80%) were obtained.

Isotope Oxygen Tracking for the Model Reaction: $^{18}O_2$ Tracking. A Schlenk tube was charged with acetophenone $\mathbf{A_1}$ (30 mg, 0.18 mmol), benzaldehyde $\mathbf{B_1}$ (26 mg, 0.19 mmol), pyrrolidine (150.0 μL, 1.8 mmol) and water (1 mL). The Schlenk tube was filled with nitrogen, which was exchanged for isotope oxygen with an isotope oxygen balloon ($^{18}O_2$). The mixture was stirred at 50 °C (oil bath) for 24 h then cooled to room temperature and quenched with 5 mL of HCl aqueous solution (30%, v/v). The purification process followed the general procedure. The isolated products $\mathbf{C_1}$ (37 mg, 69%) and $\mathbf{D_1}$ (11 mg, 22%) were subjected for HRMS analysis (Figure S1).

$H_2{}^{18}O$ Tracking. A Schlenk tube equipped with an oxygen balloon was charged with acetophenone $\mathbf{A_1}$ (30 mg, 0.18 mmol), benzaldehyde $\mathbf{B_1}$ (26 mg, 0.19 mmol), pyrrolidine (150.0 μL, 1.8 mmol) and $H_2{}^{18}O$ (1 mL). The resulting mixture was stirred at 50 °C (oil bath) for 24 h then cooled to room temperature and quenched with 5 mL of HCl aqueous solution (30%, v/v). The purification process followed the general procedure. The isolated products $\mathbf{C_1}$ (33 mg, 61%) and $\mathbf{D_1}$ (14 mg, 28%) were subjected for HRMS analysis (Figure S2).

$H_2{}^{18}O$ and $^{18}O_2$ Tracking. A Schlenk tube was charged with acetophenone $\mathbf{A_1}$ (30 mg, 0.18 mmol), benzaldehyde $\mathbf{B_1}$ (26 mg, 0.19 mmol), pyrrolidine (150.0 μL, 1.8 mmol) and $H_2{}^{18}O$ (1 mL). The Schlenk tube was filled with nitrogen, which was exchanged for isotope oxygen with an isotope oxygen balloon ($^{18}O_2$). The mixture is stirred at 50 °C (oil bath) for 24 h then cooled to room temperature and quenched with 5 mL of HCl aqueous solution (30%, v/v). The purification process followed the general procedure. The isolated products $\mathbf{C_1}$ (38 mg, 70%) and $\mathbf{D_1}$ (10 mg, 20%) were subjected for HRMS analysis (Figure S3).

Preparation of the Reference Substances. 2'-Hydroxy-4, 6'-dimethoxychalcone ($\mathbf{Y_1}$): sodium hydroxide (0.96 g, 24 mmol) was added to a solution of acetophenone $\mathbf{A_1}$ (1 g, 6 mmol), benzaldehyde $\mathbf{B_1}$ (0.86 g, 6.3 mmol) in ethanol (30 mL). The reaction mixture was stirred at room temperature for 24 h. The resulting mixture was acidified with HCl aqueous solution (30%, v/v) to pH=4. The resulting precipitate was filtered and washed with water and ethanol. The crude product was recrystallized from ethanol to afford 2'-hydroxy-4, 6'-dimethoxy chalcone $\mathbf{Y_1}$ (1.38 g, 82%) as a yellow solid.

2-3-Dihydro-5-methoxy-2-(4-methoxyphenyl)-4H-1-benzopyran-4-one ($\mathbf{Z_1}$): Sodium carbonate (1.06 g, 10 mmol) was added to a solution of 2'-hydroxy-4, 6'-dimethoxychalcone $\mathbf{Y_1}$ (0.5 g, 1.758 mmol) in MeOH (10 mL) and H_2O (10 mL). After stirring at room temperature for 3 h, the reaction mixture was diluted with water (10 mL) and extracted three times with diethyl ether (40 mL). The organic layers were combined and dried over anhydrous sodium sulfate. The organic solvent was removed in vacuo. The crude product was purified by silica gel column chromatography (PE/EA= 6/1) to afford a pale yellow solid $\mathbf{Z_1}$ (0.2 g, 35%).

2,3-Dihydro-3-hydroxy-5-methoxy-2-(4-methoxyphenyl)-4H-1-benzopyran-4-on ($\mathbf{V_1}$): The 2′-hydroxy-4, 6′-dimethoxychalcone $\mathbf{Y_1}$ (0.5 g, 1.758 mmol) was suspended in H_2O (30 mL), then sodium hydroxide (1.4 g, 35 mmol) and 30% H_2O_2 (0.9 mL, 8.79 mmol) were added at room temperature. After stirring for 2 h, the suspension was filtered and washed with water. The crude product was purified by silica gel column chromatography (PE/EA= 6/1) to afford a white solid $\mathbf{V_1}$ (0.25 g, 46%).

4-Methoxy-2-(4-methoxybenzylidene) benzofuran-3(2H)-one ($\mathbf{D_1}$): The 2'-hydroxy-4, 6'-dimethoxychalcone $\mathbf{Y_1}$ (0.5 g, 1.758 mmol) was dissolved in pyridine (10 mL), and mercuric acetate (0.843 g, 2.64 mmol) was added to the solution. The reaction mixture was stirred at 110 °C (oil bath) for 5 h then cooled to room temperature. The resulting mixture was poured into ice-cold water and acidified with HCl aqueous solution (30%, v/v) to pH=6. The resulting mixture was extracted three times with dichloromethane (20 mL), which was dried over sodium sulfate. After evaporation, the residue was on recrystallization from ethanol gave yellow needles of $\mathbf{D_1}$ (0.39 g, 85%).

***In-Situ* ^{1}H NMR Study of the Model Reaction in CD_3OD.** Pyrrolidine (30.0 μL, 0.36 mmol) was added to a solution of acetophenone $\mathbf{A_1}$ (6 mg, 0.036 mmol), benzaldehyde $\mathbf{B_1}$ (4.7 μL, 0.038 mmol) in CD_3OD (0.5 mL) and H_2O (5.2 μL, 0.288 mmol) under an atmospheric condition. The mixture is stirred at room temperature under an atmospheric condition. Then, the mixture was detected by ^{1}H NMR in a time scale manner. The ^{1}H NMR spectra resulting was time-dependent (Figure S4).

(E)-3-Methoxy-2-(3-(4-Methoxyphenyl)-1-(Pyrrolidin-1-ium-1-ylidene)allyl-2-d)phenolate ($\mathbf{E_1}$). Pyrrolidine (12.0 μL, 0.144 mmol) was added to a solution of acetophenone $\mathbf{A_1}$ (6 mg, 0.036 mmol), benzaldehyde $\mathbf{B_1}$ (4.7 μL, 0.038 mmol) in CD_3OD (0.5 mL) and H_2O (5.2 μL, 0.288 mmol) under an atmospheric condition. The reaction mixture was stirred at room temperature for 1 h then detected by NMR. The ^{1}H, $^{13}C\{^1H\}$, HSQC, HMBC NMR spectra of $\mathbf{E_1}$ were shown in Figure S5-8. ^{1}H NMR (400 MHz, CD_3OD) δ 7.73 - 7.62 (m, 2H), 7.33 (s, 1H), 7.19 (t, J = 8.3 Hz, 1H), 7.04 - 6.95 (m, 2H), 6.41 (dd, J = 8.5, 0.6 Hz, 1H), 6.21 (dd, J = 7.7 Hz, 1H), 4.22 (m, 2H), 3.87 (m, 4H), 3.71 (m, 4H), 2.36-2.19 (m, 2H), 2.16 - 1.99 (m, 2H). $^{13}C\{^1H\}$ NMR (101 MHz, CD_3OD) δ 174.8, 166.4, 163.4, 157.0, 153.2, 132.1, 131.6, 127.1, 117.3, 114.4, 114.4, 109.5, 95.1, 54.7, 54.6, 54.2, 51.9, 24.6, 23.9.

$\mathbf{E_4}$. Pyrrolidine (118.6 μL, 1.44 mmol) was added to a solution of acetophenone $\mathbf{A_1}$ (60 mg, 0.36 mmol), benzaldehyde $\mathbf{B_4}$ (44 mg, 0.36 mmol) in MeOH (5 mL) under an atmospheric condition. Then, the reaction mixture was stirred at room temperature for 1 h, intermediate $\mathbf{E_4}$ (105 mg, 90%) was generated as a precipitate, which was isolated by filtration and washed with MeOH (10 mL) three times. The ^{1}H, $^{13}C\{^1H\}$, HSQC, HMBC, NMR spectra of $\mathbf{E_4}$ were shown in Figure S9-12. ^{1}H NMR (800 MHz, CD_3OD) δ 7.50 (d, J = 8.3 Hz, 2H), 7.34 (t, J = 8.4 Hz, 1H), 7.12 (d, J = 14.6

Hz, 1H), 7.02 (d, *J* = 14.7 Hz, 1H), 6.66 (d, *J* = 8.6 Hz, 2H), 6.57 (dd, *J* = 8.5, 5.2 Hz, 2H), 4.13 – 4.06 (m, 2H), 3.77 (s, 3H), 3.66 (m, 1H), 3.55 (m, 1H), 2.23 (m, 2H), 2.07 – 2.01 (m, 2H). $^{13}C\{^1H\}$ NMR (201 MHz, CD_3OD) δ 161.8, 161.7, 161.5, 156.9, 155.6, 144.5, 138.8, 132.4, 122.4, 118.6, 110.3, 108.8, 100.1, 55.0, 53.4, 51.2, 24.5, 24.1. HRMS (ESI) m/z: $[M+H]^+$ calcd for $C_{20}H_{21}NO_3^+$ 324.1594; found 324.1594. Elementary analysis: calcd for $C_{40}H_{44}N_2O_7$: C, 72.27; N, 4.24; H, 6.67; found: C, 72.26; N, 4.41; H, 6.511. All data indicate that this precipitate is an aggregate of **E_4**, with a formula of **$2E_4.H_2O$.**

(E)-1-(1-(2-Hydroxy-6-methoxyphenyl)-3-(4-Hydroxyphenyl)allylidene)pyrrolidin-1-ium chloride (E_4-A). A NMR tube was charged with **E_4** (10 mg), CD_3OD (0.5 mL), and HCl aqueous solution (36%, v/v) (20 μL). Then, the resulting mixture was detected by NMR (Figure S13-14). ^1H NMR (400 MHz, CD_3OD) δ 7.66 (d, *J* = 8.7 Hz, 2H), 7.48 (t, *J* = 8.4 Hz, 1H), 7.37 (d, *J* = 15.1 Hz, 1H), 7.17 (d, *J* = 15.1 Hz, 1H), 6.90 (d, *J* = 8.7 Hz, 2H), 6.75 (t, *J* = 7.8 Hz, 2H), 4.36 - 4.24 (m, 2H), 3.83 (s, 3H), 3.78 - 3.61 (m, 2H), 2.30 (p, *J* = 6.9 Hz, 2H), 2.11 (p, *J* = 6.9 Hz, 2H). $^{13}C\{^1H\}$ NMR (101 MHz, CD_3OD) δ 171.0, 162.9, 156.8, 155.4, 154.8, 133.5, 132.7, 125.5, 116.2, 115.4, 108.7, 107.4, 102.6, 55.5, 54.7, 52.7, 24.5, 24.0. HRMS (ESI) m/z: $[M+H]^+$ calcd for $C_{20}H_{21}NO_3$ 324.1521; found 324.1642.

(E)-1-(3-(4-Hydroxy-3,5-dimethoxyphenyl)-1-(2-Hydroxy-6-methoxyphenyl)allylidene)pyrrolidin-1-ium chloride (E_{13}.HCl). Pyrrolidine (118.6 μL, 1.44 mmol) was added to a solution of acetophenone **A_1** (60 mg, 0.36 mmol), benzaldehyde **B_{13}** (60 mg, 0.36 mmol) in MeOH (5 mL) under an atmospheric condition. Then, the reaction mixture was stirred at room temperature for 4 h. the mixture was poured into ice-cold water and acidified with HCl aqueous solution (30%, v/v) to pH=4. The mixture was extracted with DCM (3 × 100 mL), the organic layer was combined and dried over sodium sulfate, filtered and concentrated. Yellow enimine salt intermediate **E_{13}.HCl** (121 mg, 80%) were obtain. The ^1H, $^{13}C\{^1H\}$ NMR spectra and single-crystal structure of **E_{13}.HCl** were shown in Figure S15-17. ^1H NMR (400 MHz, D_2O) δ 7.48 (t, *J* = 8.4 Hz, 1H), 6.87 (s, 2H), 6.70 (d, *J* = 8.0 Hz, 1H), 6.65 (d, *J* = 12.0 Hz, 1H), 6.51 (s, 2H), 3.99 (m, 2H), 3.63 (s, 9H), 3.56 (m, 2H), 2.14 (m, 2H), 1.93 (m, 2H). $^{13}C\{^1H\}$ NMR (101 MHz, D_2O) δ 167.0, 156.4, 155.7, 153.5, 147.4, 139.8, 133.9, 125.0, 115.7, 109.0, 107.6, 103.8, 56.0, 55.1, 52.7, 24.5, 24.0. HRMS (ESI) m/z: $[M]^+$ calcd for $C_{22}H_{26}NO_5$ 384.1805; found 384.1840. Elementary analysis: calcd for $C_{44}H_{54}Cl_2N_2O_{11}$: C, 61.61; N, 3.27; H, 6.35; Cl, 8.27 found: C, 61.82; N, 2.81; H, 6.24; Cl, 8.12. All data indicate that this precipitate is an aggregate of **E_{13}HCl**, with a formula of **$2E_{13}$ HCl.H_2O.**

X-ray crystallographic analysis of E_{13}.HCl. In a sealable bottle, the dried solids of **E_{13}HCl** (20 mg) were dissolved in 10 mL methanol and 1mL water. The X-ray-quality crystals were obtained from the capped bottle after one week. The X-ray crystallographic analysis of the intermediate **E_{13}.HCl** was shown in Figure S17.

The Reaction of E_4 with Pyrrolidine. Pyrrolidine (1 ml, 12.6 mmol) was added to a suspending solution of **E_4** (40 mg, 0.126 mmol) in different solvents (10 mL) (H_2O, CH_3OH, CH_3CN) under an atmospheric condition. The resulting mixture was stirred at room temperature for 24 h. The mixture was poured into ice-cold water and acidified with HCl aqueous solution (30%, v/v) to pH=4. The produced precipitate was filtered and then washed with water and ethanol. The crude product were recrystallized from ethanol to afford **C_4**. The flavonol **C_4** was respectively generated with 80% yield in water, 40% yield in methanol, and trace **C_4** in acetonitrile.

The Reaction of E_4 with H_2O_2.30% H_2O_2 (28 μL, 0.9 mmol) was added to a solution of **E_4** (30 mg, 0.09 mmol) in water (2 mL). The resulting mixture was stirred at room temperature for 30 min. Then, dihydrogenflavonol (**V_4**) **(**21 mg, 80%) was generated as a precipitate, which was isolated by filtration. The ^1H and $^{13}C\{^1H\}$ NMR spectra of **V_4** were shown in Figure S18-19. ^1H NMR (400 MHz, DMSO-*d6*) δ 9.55 (s, 1H), 7.48 (t, *J* = 8.3 Hz, 1H), 7.32 (d, *J* = 8.4 Hz, 1H), 6.79 (d, *J* = 8.4 Hz, 1H), 5.40 (d, *J* = 5.0 Hz, 1H), 5.07 (d, *J* = 11.4 Hz, 1H), 4.48 (dd, *J* = 11.3, 5.0 Hz, 1H), 3.84 (s, 2H). $^{13}C\{^1H\}$ NMR (101 MHz, DMSO-d_6) δ 192.5, 162.5, 160.6, 158.1, 136.7, 129.8, 128.1, 115.3, 109.8, 109.7, 104.8, 82.9, 73.3, 56.4. HRMS (ESI) m/z: $[M+Na]^+$ calcd for $C_{16}H_{14}O_5Na$ 309.0733; found 309.0734.

The Reaction of E_{13}.HCl with Pyrrolidine. Pyrrolidine (1 mL, 12.6 mmol) was added to a suspending solution of **E_{13}.HCl** (52 mg, 0.126 mmol) in CH_3CN (10 mL) under an atmospheric condition. The resulting mixture was stirred at room temperature for 24 h then cooled to room temperature. The mixture was poured into ice-cold water and acidified with HCl aqueous solution (30%, v/v) to pH=4. Then, the mixture extracted with DCM (100 mL) three times, the organic layer was combined and dried over sodium sulfate, filtered and concentrated. The crude product was purified by flash silica gel column chromatography to give **D_{13}** (12 mg, 30%) as a yellow solid.

The Reaction of E_{13}.HCl with H_2O_2.30% H_2O_2 (51.0 μL, 2.4 mmol) and sodium hydroxide (9.6 mg, 0.24 mmol) was added to a solution of **E_{13}.HCl** (100 mg, 0.24mmol) in H_2O (5.0 mL) under an atmospheric condition. The resulting mixture was stirred at room temperature for 2 h. Dihydroflavonol (**V_{13}**) **(**21 mg, 80%) was generated as a precipitate, which was isolated by filtration. The ^1H, $^{13}C\{^1H\}$ NMR spectra of **V_{13}** were shown in Figure S20-21. ^1H NMR (400 MHz, $CDCl_3$) δ 7.48 (t, *J* = 8.4 Hz, 1H), 6.82 (s, 2H), 6.67 (d, *J* = 8.3 Hz, 1H), 6.61 (d, *J* = 8.3 Hz, 1H), 5.66 (s, 1H), 5.00 (d, *J* = 12.3 Hz, 1H), 4.55 (d, *J* = 12.3 Hz, 1H), 4.05 (s, 1H), 3.99 (s, 3H), 3.96 (s, 6H). $^{13}C\{^1H\}$ NMR (101 MHz, $CDCl_3$) δ 192.6, 163.0, 160.7, 147.1, 137.2, 135.6, 127.3, 110.1, 108.5, 104.4, 104.2, 83.6, 73.1, 56.4, 56.3. HRMS (ESI) m/z: $[M+Na]^+$ calcd for $C_{18}H_{18}NaO_7$ 369.0945; found 369.0945.

UV-visible Spectra Characterization of E_4. The stock solution with the final concentration of 5×10^{-4} M was prepared by dissolving 16 mg of **E_4** in 50mL methanol, transfer the solution to 100 mL volumetric flask and set the volume to the scale for use. Taking o.1 mL of stock solution using a Hamilton syringe into the colourimeter, then adding 3 mL different solvents (water, acetonitrile) and different concentrations of pyrrolidine, After each of addition, the UV-vis absorption was measured in the wavelength range of 300-600. All the titration experiments were carried out on a Pgeneral TU-1900 spectrometer at 298K. UV-vis absorption spectra of **E_4** (1.7×10^{-5} M), **E_4** with equal molar HCl (break line) and **E_4** in the presence of 0.2-10 equivalents of pyrrolidine (plain lines) in water and acetonitrile were recorded, respectively (Figure S22, (1), (3)).

UV-visible Spectra Characterization of E_{13}.HCl. The stock solution with the final concentration of 5×10^{-4} M was prepared by dissolving 10.5 mg of **E_{13}.HCl** in 20 mL methanol, transfer the solution to 50 mL volumetric flask and set the volume to the scale for use. Taking o.2 mL of stock solution using a Hamilton syringe into the colourimeter, then adding 3 mL different solvents (water, acetonitrile) and different concentrations of pyrrolidine, After each of addition, the UV-vis absorption was measured in the wavelength range of 300-600. All the titration experiments were carried out on a Pgeneral TU-1900 spectrometer at 298K. The UV-vis spectra of **E_{13}.HCl** (3.4×10^{-5} M, break line) and **E_{13}HCl** with an increasing pyrrolidine amount from 0.2 to 10 equivalents in water and acetonitrile were recorded (Figure S23, (1), (3)).

LCMS Study for the Model Reaction under $^{18}O_2$. Method: Column: Waters X-Bridge-Shield-RP-C18 50 mm*4.6 mm 3.5 µm; Mobile Phase: A: 0.05% TFA Water B: 0.05% TFA CAN; Gradient: B from 10% to 100% for 4.0 min and hold 100% for 1.0 min; Flow Rate: 2.5 mL/min; Column Temperature: 40 °C. **Assay conditions:** A Schlenk tube was charged with acetophenone **A_1** (30 mg, 0.18 mmol), benzaldehyde **B_1** (26 mg, 0.19 mmol), pyrrolidine (150.0 µL, 1.8 mmol) and water (2 mL). The Schlenk tube is filled with nitrogen, which is exchanged for isotope oxygen with an isotope oxygen balloon ($^{18}O_2$). The mixture was stirred at 50 °C (oil bath) for 3 h and examined by LC-HRMS (Figure S24).

LCMS Study for the Reaction of E_4 with Pyrrolidine in Water. Method: Column: Waters X-Bridge-Shield-RP-C18 50 mm*4.6 mm 3.5 um; Mobile Phase: A: Water B: MeOH; Gradient: B from 10% to 100% for 4.0 min and hold 100% for 1.0 min; Flow Rate: 2.5 mL/min; Column Temperature: 40 °C. **Assay conditions**: Pyrrolidine (26.0 µL, 0.31 mmol) was added to a solution of intermediate **E_4** (10 mg, 0.031 mmol) in H_2O (2 mL). The mixture was stirred at room temperature under an atmospheric condition. The reaction mixture was examined by LCMS at 0min, 40 min, 2h, 4h, 8h, 12h, 24h. (Figure S25).

LCMS Study for the Reaction of E_{13}.HCl with Pyrrolidine in Acetonitrile. Method: Column: Waters X-Bridge-Shield-RP-C18 50 mm*4.6 mm 3.5 um; Mobile Phase: A: Water B: MeOH; Gradient: B from 10% to 100% for 4.0 min and hold 100% for 1.0 min; Flow Rate: 2.5 mL/min; Column Temperature: 40 °C. **Assay conditions**: Pyrrolidine (20 µL, 0.24 mmol) was added to a solution of intermediate **E_{13}.HCl** (10 mg, 0.024 mmol) in CH_3CN (2 mL). The mixture was stirred at room temperature under an atmospheric condition. The reaction mixture was examined by LCMS at 0 h, 2 h, 4 h, 8 h, 12 h, and 24 h. (Figure S26).

Calculation Methods. Density functional theory (DFT) calculations were performed with Gaussian 03 program.[27] The M06-2X functional by Zhao and Truhlar was used, with the standard 6-31+G (d) basis set. The geometries of reactants, transition states (TS), and products were fully optimized, followed by vibrational frequency calculations at the same levels of theory to obtain the zero-point energies (ZPE) and verify whether it is a minimum or a transition state on the potential energy surfaces (PES).[28] To estimate the bulk solvent effects on the reaction, all structures were optimized in methanol solvent with the polarized continuum model using the integral equation formalism variant (IEFPCM).[29] The temperature-dependent enthalpy corrections and the entropy effects are computed at 298K and 1 atmosphere of pressure. As shown in Figure S27, the reaction would prefer to the reaction channel via transition state TS-A for the process via TS-A has lower Gibbs free energy barrier. The transition state TS-B is 3.3 kcal mol^{-1} less stable than TS-A. Thus, the product with five-membered ring structures would be the major product.

1-[2-Hydroxy-4,6-bis(Methoxymethoxy)phenyl]ethanone (A_4): Colorless oil; yield 76%; ^{1}H NMR (400 MHz, $CDCl_3$) δ 13.73 (s, 1H), 6.26 (dd, *J* = 6.5, 2.3 Hz, 2H), 5.26 (s, 2H), 5.18 (s, 2H), 3.53 (s, 3H), 3.48 (s, 3H), 2.66 (s, 3H). $^{13}C\{^1H\}$ NMR (101 MHz, $CDCl_3$) δ 203.2, 166.8, 163.5, 160.4, 106.9, 97.1, 94.5, 94.0, 56.7, 56.4, 33.0. HRMS (ESI) m/z: $[M+Na]^+$ calcd for $C_{12}H_{16}NaO_6$ 279.0839; found 279.0841.

3-Hydroxy-5-methoxy-2-(4-Methoxyphenyl)-4H-chromen-4-one (C_1): Yellow solid; yield: 63%; mp: 168-170 °C (EtOH-H_2O); ^{1}H NMR (400 MHz, $CDCl_3$) δ 8.23 (d, *J* = 8.8 Hz, 2H), 7.59 (t, *J* = 8.3 Hz, 1H), 7.37 (s, 1H), 7.16 (d, *J* = 8.5 Hz, 1H), 7.06 (d, *J* = 8.8 Hz, 2H), 6.80 (d, *J* = 8.1 Hz, 1H), 4.05 (s, 3H), 3.91 (s, 3H). $^{13}C\{^1H\}$ NMR (101 MHz, $CDCl_3$) δ 172.7, 160.9, 159.5, 157.2, 143.0, 137.9, 133.7, 129.2, 123.4, 114.1, 111.4, 110.3, 104.9, 56.5, 55.4. HRMS (ESI) m/z: $[M+Na]^+$ calcd for $C_{17}H_{14}NaO_5$ 321.0733; found 321.0720.

2-(4-(Dimethylamino)phenyl)-3-hydroxy-5-methoxy-4H-chromen-4-one (C_2): Yellow solid; yield: 85%; mp: 170-172 °C (CH_3OH-H_2O); ^{1}H NMR (400 MHz, $CDCl_3$) δ 8.18 (d, *J* = 9.1 Hz, 2H), 7.55 (t, *J* = 8.4 Hz, 1H), 7.34 (s, 1H), 7.15 (d, *J* = 8.5 Hz, 1H), 6.77-6.83 (m, 3H), 4.04 (s, 3H), 3.08 (s, 6H). $^{13}C\{^1H\}$ NMR (101 MHz, $CDCl_3$) δ 172.2, 159.4, 157.0, 151.2, 144.3, 137.2, 133.2, 128.9, 118.1, 111.6, 110.3, 104.7, 56.4, 40.1. HRMS (ESI) m/z: $[M+Na]^+$ calcd for $C_{18}H_{17}NNaO_4$ 334.1050; found 334.1045.

3-Hydroxy-5-methoxy-2-(p-Tolyl)-4H-chromen-4-one (C_3): Yellow solid; yield: 60%; mp: 165-167 °C (CH_3OH-H_2O); ^{1}H NMR (600 MHz, $CDCl_3$) δ 8.14 (d, *J* = 8.3 Hz, 2H), 7.58 (t, *J* = 8.4 Hz, 1H), 7.37 (s, 1H), 7.33 (d, *J* = 8.2 Hz, 2H), 7.16 (d, *J* = 8.5 Hz, 1H), 6.79 (d, *J* = 8.2 Hz, 1H), 4.03 (s, 3H), 2.43 (s, 3H). $^{13}C\{^1H\}$ NMR (150 MHz, $CDCl_3$) δ 172.8, 159.6, 157.3, 142.9, 140.3, 138.4, 133.8, 129.3, 128.2, 127.4, 111.5, 110.3, 104.9, 56.4, 21.5. HRMS (ESI) m/z: $[M+Na]^+$ calcd for $C_{17}H_{14}NaO_4$ 305.0784; found 305.0773.

3-Hydroxy-5-methoxy-2-(4-Hydroxyphenyl)-4H-chromen-4-one (C_4): Yellow needles; yield: 85%; mp: 240-242 °C (CH_3OH-H_2O); ^{1}H NMR (400 MHz, DMSO-d_6) δ 10.08 (s, 1H), 8.95 (s, 1H), 8.07 (d, *J* = 8.9 Hz, 2H), 7.66 (t, *J* = 8.4 Hz, 1H), 7.24 (d, *J* = 8.3 Hz, 1H), 6.99 – 6.89 (m, 3H), 3.90 (s, 3H), 3.38 (s, 14H). $^{13}C\{^1H\}$ NMR (101 MHz, DMSO-d_6) δ 172.2, 159.5, 159.3, 156.8, 143.4, 138.3, 134.2, 129.6, 122.2, 115.9, 112.1, 110.4, 106.1, 56.6. HRMS (ESI) m/z: $[M+H]^+$ calcd for $C_{16}H_{13}O_5$ 285.0760; found 285.0757.

3-Hydroxy-5-methoxy-2-phenyl-4H-chromen-4-one (C_5): Yellow solid; yield: 35%; mp: 169-171 °C (CH_3OH-H_2O); ^{1}H NMR (400 MHz, Acetone-d_6) δ 8.33 – 8.27 (m, 2H), 8.11 (s, 1H), 7.71 (t, *J* = 8.4 Hz, 1H), 7.59 (t, *J* = 7.5 Hz, 2H), 7.51 (t, *J* = 7.3 Hz, 1H), 7.28 (d, *J* = 7.8 Hz, 1H), 6.98 (d, *J* = 8.1 Hz, 1H), 3.98 (s, 3H). $^{13}C\{^1H\}$ NMR (101 MHz, Acetone-d_6) δ 172.1, 159.7, 157.3, 141.6, 138.9, 134.2, 131.4, 129.6, 128.5, 127.3, 111.5, 110.0, 105.5, 55.7. HRMS (ESI) m/z: $[M+Na]^+$ calcd for $C_{16}H_{12}NaO_4$ 291.0628; found 291.0619.

2-(4-Chlorophenyl)-3-hydroxy-5-methoxy-4H-chromen-4-one (C_6): Yellow solid; yield: 10%; mp: 195-197 °C (CH_3OH-H_2O); ^{1}H NMR (600 MHz, $CDCl_3$) δ 8.22 (d, *J* = 8.7 Hz, 2H), 7.63 (t, *J* = 8.4 Hz, 1H), 7.52 (d, *J* = 8.7 Hz, 2H), 7.46 (s, 1H), 7.18 (d, *J* = 8.5 Hz, 1H), 6.83 (d, *J* = 8.3 Hz, 1H), 4.06 (s, 3H). $^{13}C\{^1H\}$ NMR (150 MHz, $CDCl_3$) δ 172.8, 159.7, 157.3, 141.4, 138.7, 135.9, 134.1, 129.5, 128.9, 128.7, 111.4, 110.3, 105.1, 56.5. HRMS (ESI) m/z: $[M+Na]^+$ calcd for $C_{16}H_{11}{}^{35}ClNaO_4$ 325.0238; found 325.0229; $[M+Na]^+$ calcd for $C_{16}H_{11}{}^{37}ClNaO_4$ 327.0227; found 327.0227.

3-Hydroxy-5-methoxy-2-(m-tolyl)-4H-chromen-4-one (C_9): White solid; yield: 42%; mp: 142-144 °C (CH_3OH-H_2O); ^{1}H NMR (400 MHz, Acetone-d_6) δ 8.10 (d, *J* = 9.3 Hz, 2H), 7.71 (t, *J* = 8.4 Hz, 1H), 7.46 (t, *J* = 7.7 Hz, 1H), 7.33 (d, *J* = 7.6 Hz, 1H), 7.27 (d, *J* = 8.5 Hz, 1H), 6.97 (d, *J* = 8.2 Hz, 1H), 3.98 (s, 3H), 2.46 (s, 3H). $^{13}C\{^1H\}$ NMR (101 MHz, Acetone-d_6) δ 172.0, 159.7, 157.3, 141.8, 138.8, 138.0, 134.1, 131.3, 130.4, 128.4, 127.7, 124.6, 115.9, 111.4, 110.0, 105.4, 55.7. HRMS (ESI) m/z: $[M+Na]^+$ calcd for $C_{17}H_{14}NaO_4$ 305.0784; found 305.0772.

3-Hydroxy-5-methoxy-2-(3-Hydroxyphenyl)-4H-chromen-4-one (C_{10}): Yellow solid; yield: 52%; mp: 267-269 °C (EtOH-H_2O); ^{1}H NMR (400 MHz, DMSO-d_6) δ 9.73 (s, 1H), 9.19 (s, 1H), 7.74 – 7.57 (m, 3H), 7.36 (t, *J* = 8.0 Hz, 1H), 7.23 (d, *J* = 8.4 Hz, 1H), 6.95 (d, *J* = 8.2 Hz, 1H), 6.89 (dd, *J* = 8.0, 2.4 Hz, 1H), 3.91 (s, 3H). $^{13}C\{^1H\}$ NMR (101 MHz, DMSO-d_6) δ 172.5, 159.6, 157.8, 156.9, 142.5, 139.6, 134.6, 132.7, 130.0, 118.5, 117.2, 114.6, 112.1, 110.4, 106.2, 56.7. HRMS (ESI) m/z: $[M+Na]^+$ calcd for $C_{16}H_{12}NaO_5$ 307.0577; found 307.0575.

2-(3-Methoxy-4-hydroxyphenyl)-3-hydroxy-5-methoxy-4H-chromen-4-one (C_{11}): Yellow needles; yield: 83%; mp: 248-250 °C (EtOH-H_2O); ^{1}H NMR (400 MHz, DMSO-d_6) δ 9.71 (s, 1H), 8.99 (s, 1H), 7.79 (d, J = 2.0 Hz, 1H), 7.72 (dd, J = 8.5, 2.0 Hz, 1H), 7.67 (t, J = 8.4 Hz, 1H), 7.28 (d, J = 8.5 Hz, 1H), 6.97 (d, J = 7.7 Hz, 1H), 3.90 (s, 3H), 3.86 (s, 3H). ^{13}C{^{1}H} NMR (101 MHz, DMSO-d_6) δ 172.2, 159.5, 156.8, 148.9, 147.9, 143.2, 138.5, 134.2, 122.6, 121.7, 116.0, 112.0, 111.8, 110.5, 106.1, 56.6, 56.2. HRMS (ESI) m/z: $[M+H]^+$ calcd for $C_{17}H_{15}O_6$ 315.0863; found 315.0859.

2-(3,4-Dimethoxyphenyl)-3-hydroxy-5-methoxy-4H-chromen-4-one (C_{12}): Yellow solid; yield: 61%; mp: 175-177 °C (CH_3OH-H_2O); ^{1}H NMR (400 MHz, $CDCl_3$) δ 7.92 – 7.80 (m, 2H), 7.60 (t, J = 8.4 Hz, 1H), 7.43 (s, 1H), 7.18 (d, J = 8.5 Hz, 1H), 7.04 (d, J = 9.1 Hz, 1H), 6.81 (d, J = 8.2 Hz, 1H), 4.06 (s, 3H), 4.01 (s, 3H), 3.99 (s, 3H). ^{13}C{^{1}H} NMR (101 MHz, $CDCl_3$) δ 172.7, 159.5, 157.2, 150.5, 148.8, 142.8, 138.0, 133.8, 123.6, 121.0, 110.9, 110.4, 105.0, 56.5, 56.0. HRMS (ESI) m/z: $[M+Na]^+$ calcd for $C_{18}H_{16}NaO_6$ 351.0839; found 351.0827.

3-Hydroxy-2-(4-Hydroxy-3,5-dimethoxyphenyl)-5-methoxy-4H-chromen-4-one (C_{13}): Yellow solid; yield: 50%; mp: 178-180 °C (EtOH-H_2O) ^{1}H NMR (400 MHz, $CDCl_3$) δ 7.64 – 7.56 (m, 3H), 7.19 (d, J = 8.5 Hz, 1H), 6.85 – 6.80 (m, 1H), 5.87 (s, 1H), 4.06 (s, 3H), 4.03 (s, 6H). ^{13}C{^{1}H} NMR (101 MHz, $CDCl_3$) δ 172.6, 159.6, 157.1, 147.0, 142.8, 138.0, 136.7, 133.8, 122.1, 111.4, 111.4, 110.3, 105.0, 104.8, 77.3, 77.2, 77.0, 76.7, 56.5, 56.5. HRMS (ESI) m/z: $[M+Na]^+$ calcd for $C_{18}H_{16}NaO_7$ 367.0794; found 367.0793.

3-Hydroxy-5-methoxy-2-(Thiophen-2-yl)-4H-chromen-4-one (C_{14}): Yellow solid; yield: 76%; mp: 204-206 °C (CH_3OH-H_2O); ^{1}H NMR (400 MHz, $CDCl_3$) δ 7.98 (d, J = 3.8 Hz, 1H), 7.60 (dd, J = 10.2, 6.7 Hz, 2H), 7.25 (m, 1H), 7.16 (d, J = 8.5 Hz, 1H), 6.81 (d, J = 8.2 Hz, 1H), 4.05 (s, 3H). ^{13}C{^{1}H} NMR (101 MHz, $CDCl_3$) δ 172.1, 159.6, 157.0, 140.3, 136.5, 133.9, 132.8, 129.4, 128.8, 128.1, 111.7, 110.3, 105.2, 56.5. HRMS (ESI) m/z: $[M+Na]^+$ calcd for $C_{14}H_{10}NaO_4S$ 297.0192; found 297.0182.

5-Fluoro-3-hydroxy-2-(4-Methoxyphenyl)-4H-chromen-4-one (C_{15}): Yellow solid; yield: 81%; mp: 198-200 °C (CH_3OH-H_2O); ^{1}H NMR (400 MHz, $CDCl_3$) δ 8.24 (d, J = 8.6 Hz, 2H), 7.64 (dd, J = 13.4, 7.8 Hz, 1H), 7.41 (d, J = 8.2 Hz, 1H), 6.99-7.23 (m, 4H), 3.93 (s, 3H). ^{13}C{^{1}H} NMR (101 MHz, $CDCl_3$) δ 171.3 (d, J=1.01 Hz), 161.2, 160.3 (d, J = 264.62 Hz), 159.0, 156.1, 156.1, 144.5, 137.9, 133.3 (d, J = 11.11 Hz), 129.5, 123.0, 114.2, 114.1, 110.7 (d, J = 19.19Hz), 55.4 HRMS (ESI) m/z: $[M+Na]^+$ calcd for $C_{16}H_{11}FNaO_4$ 309.0534; found 309.0523.

5-Fluoro-3-hydroxy-2-(3,4,5-Trimethoxyphenyl)-4H-chromen-4-one(C_{16}): Yellow solid; yield: 78%; mp: 187-189 °C (EtOH); ^{1}H NMR (400 MHz, $CDCl_3$) δ 7.66 (td, J = 8.3, 5.6 Hz, 1H), 7.54 (s, 2H), 7.43 (d, J = 8.6 Hz, 1H), 7.25 (s, 1H), 7.10 (dd, J = 10.3, 8.1 Hz, 1H), 3.99 (s, 6H), 3.97 (s, 3H). ^{13}C{^{1}H} NMR (101 MHz, CDCl3) δ 171.5, 160.3 (d, J= 265.63 Hz), 156.1, 156.1, 153.3, 143.9, 140.1, 138.4, 133.6 (d, J = 10.1 Hz), 125.7, 114.2 (d, J = 4.04 Hz), 111.3 (d, J = 11.11Hz), 110.9 (d, J = 20.2 Hz), 105.4, 61.0, 56.3 HRMS (ESI) m/z: $[M+H]^+$ calcd for $C_{18}H_{16}FO_6$ 347.0925; found 347.0937.

5,7-Dimethoxy-3-hydroxy-2-(4-Methoxyphenyl)-4H-chromen-4-one (C_{17}): Yellow solid; yield: 85%; mp: 155-157 °C (EtOH-H_2O); ^{1}H NMR (400 MHz, $CDCl_3$) δ 8.19 (d, J = 9.0 Hz, 2H), 7.38 (s, 1H), 7.04 (d, J = 9.0 Hz, 2H), 6.56 (d, J = 2.1 Hz, 1H), 6.36 (d, J = 2.1 Hz, 1H), 3.99 (s, 3H), 3.93 (s, 3H), 3.90 (s, 3H). ^{13}C{^{1}H} NMR (101 MHz, $CDCl_3$) δ 171.9, 164.3, 160.6, 160.5, 158.8, 142.2, 137.4, 128.9, 123.6, 114.0, 106.2, 95.7, 92.4, 56.4, 55.8, 55.4. HRMS (ESI) m/z: $[M+Na]^+$ calcd for $C_{16}H_{12}NaO_5$ 307.0577; found 307.0575.

2-(4-(Dimethylamino)phenyl)-5,7-dimethoxy-3-hydroxy-4H-chromen-4-one (C_{18}): Yellow solid; yield: 90%; mp: 210-212 °C (EtOH-H_2O); ^{1}H NMR (400 MHz, $CDCl_3$) δ8.13 (d, J = 9.2 Hz, 1H), 7.34 (s, 1H), 6.80 (d, J = 9.2 Hz, 1H), 6.55 (d, J = 2.2 Hz, 1H), 6.34 (d, J = 2.2 Hz, 1H), 3.99 (s, 3H), 3.92 (s, 3H), 3.07 (s, 6H). ^{13}C{^{1}H} NMR (101 MHz, $CDCl_3$) δ 171.6, 163.9, 160.4, 158.7, 151.0, 143.5, 136.7, 128.5, 118.3, 111.6, 106.3, 95.4, 92.4, 56.4, 55.8, 40.1. HRMS (ESI) m/z: $[M+Na]^+$ calcd for $C_{19}H_{19}NNaO_5$ 364.1155; found 364.1155.

5,7-Dimethoxy-3-hydroxy-2-(4-Hydroxyphenyl)-4H-chromen-4-one (C_{19}): Yellow solid; yield: 82%; mp: 263-265 °C (EtOH-H_2O); ^{1}H NMR (400 MHz, DMSO-d_6) δ 10.01 (s, 1H), 8.78 (s, 1H), 8.06 (d, J = 8.8 Hz, 2H), 6.94 (d, J = 8.8 Hz, 2H), 6.82 (d, J = 2.1 Hz, 1H), 6.48 (d, J = 2.1 Hz, 1H), 3.91 (s, 3H), 3.87 (s, 3H). ^{13}C{^{1}H} NMR (101 MHz, DMSO-d_6) δ 171.5, 164.1, 160.6, 159.1, 158.5, 142.7, 137.9, 129.3, 122.3, 115.9, 106.7, 96.1, 93.2, 56.6, 56.4. HRMS (ESI) m/z: $[M+Na]^+$ calcd for $C_{17}H_{14}NaO_6$ 337.0683; found 337.0683.

5,7-Dimethoxy-3-hydroxy-2-(3-Hydroxyphenyl)-4H-chromen-4-one (C_{20}): Yellow solid; Yield: 68%; mp: 267-269 °C (EtOH-H_2O); ^{1}H NMR (400 MHz, DMSO-d_6) δ 7.66 (s, 1H), 7.63 (d, J = 7.9 Hz, 1H), 7.34 (t, J = 8.0 Hz, 1H), 6.88 (d, J = 7.9 Hz, 1H), 6.80 (s, 1H), 6.49 (s, 1H), 3.91 (s, 3H), 3.88 (s, 3H). ^{13}C{^{1}H} NMR (101 MHz, DMSO-d_6) δ 171.7, 164.3, 160.6, 158.6, 157.8, 141.8, 139.2, 132.8, 129.9, 118.2, 117.0, 114.4, 106.7, 96.2, 93.1, 56.7, 56.4. HRMS (ESI) m/z: $[M+Na]^+$ calcd for $C_{17}H_{14}NaO_6$ 337.0681; found 337.0683.

2-(3,4-Dimethoxyphenyl)-3-hydroxy-5,7-dimethoxy-4H-chromen-4-one(C_{21}): Yellow solid; Yield: 85%; mp: 267-269 °C (EtOH-H_2O); ^{1}H NMR (400 MHz, $CDCl_3$) δ 7.81 (d, J = 8.5 Hz, 2H), 7.43 (s, 1H), 7.01 (d, J = 8.2 Hz, 1H), 6.55 (s, 1H), 6.36 (s, 1H), 4.00 (s, 3H), 3.99 (s, 3H), 3.97 (s, 3H), 3.94 (s, 3H). ^{13}C{^{1}H} NMR (101 MHz, $CDCl_3$) δ 171.9, 164.3, 160.5, 158.8, 150.3, 148.8, 142.1, 137.5, 123.8, 120.6, 110.9, 110.4, 106.2, 95.7, 92.4, 56.4, 56.0, 55.9, 55.8. HRMS (ESI) m/z: $[M+Na]^+$ calcd for $C_{19}H_{18}NaO_7$ 381.0945; found 381.0935.

3-Hydroxy-2-(4-Hydroxy-3-Methoxyphenyl)-5,7-dimethoxy-4H-chromen-4-one (C_{22}): Yellow solid; Yield: 80%; mp: 267-269 °C (EtOH-H_2O); ^{1}H NMR (400 MHz, DMSO-d_6) δ 9.26 (s, 1H), 8.84 (s, 1H), 7.71 (d, J = 2.1 Hz, 1H), 7.66 (dd, J = 8.6, 2.0 Hz, 1H), 7.08 (d, J = 8.7 Hz, 1H), 6.78 (d, J = 1.7 Hz, 1H), 6.48 (d, J = 1.7 Hz, 1H), 3.91 (s, 3H), 3.87 (s, 3H), 3.86 (s, 3H). ^{13}C{^{1}H} NMR (101 MHz, DMSO-d_6) δ 171.5, 164.1, 160.6, 158.5, 149.3, 146.7, 142.3, 138.3, 124.2, 119.4, 114.7, 112.3, 106.7, 96.1, 93.1, 56.6, 56.4, 56.1. HRMS (ESI) m/z: $[M+H]^+$ calcd for $C_{18}H_{17}O_7$ 345.0969; found 345.0965.

5,7-Bis(Methoxymethoxy)-2-(4-(Dimethylamino) phenyl)-3-hydroxy-4H-chromen-4-one (C_{23}): Yellow solid; yield: 88%; mp: 170-172 °C (EtOH-H_2O); ^{1}H NMR (400 MHz, $CDCl_3$) δ 8.21 (d, J = 9.0 Hz, 2H), 7.34 (s, 1H), 7.05 (d, J = 9.0 Hz, 2H), 6.87 (d, J = 2.2 Hz, 1H), 6.76 (d, J = 2.2 Hz, 1H), 5.40 (s, 2H), 5.29 (s, 2H), 3.91 (s, 3H), 3.60 (s, 3H), 3.55 (s, 3H). ^{13}C{^{1}H} NMR (101 MHz, $CDCl_3$) δ 171.9, 161.5, 160.7, 158.3, 157.8, 142.6, 137.4, 129.0, 123.5, 114.0, 107.4, 100.7, 96.6, 95.3, 94.4, 56.6, 56.6, 55.4. HRMS (ESI) m/z: $[M+H]^+$ calcd for $C_{20}H_{21}NaO_8$ 411.1050; found 411.1047.

3-Hydroxy-2-phenyl-4H-chromen-4-one (C_{24}): Yellow solid; yield: 78%; mp: 170-172 °C (EtOH-H_2O); ^{1}H NMR (400 MHz, $CDCl_3$) δ 8.29 (d, J = 7.5 Hz, 3H), 7.78 - 7.71 (m, 1H), 7.66 - 7.54 (m, 3H), 7.54 - 7.41 (m, 2H), 7.06 (s, 1H). ^{13}C{^{1}H} NMR (101 MHz, $CDCl_3$) δ 173.5, 155.4, 144.9, 138.5, 133.7, 131.1, 130.2, 128.6, 127.8, 125.5, 124.5, 120.7, 118.3. HRMS (ESI) m/z: $[M-H]^-$ calcd for $C_{15}H_9O_3$ 237.0547; found 237.0549.

3-Hydroxy-2-(p-Tolyl)-4H-chromen-4-one (C_{25}): Yellow solid; yield: 80%; mp: 191-193 °C (EtOH-H_2O); ^{1}H NMR (400 MHz,

$CDCl_3$) δ 8.25 (dd, *J* = 8.0, 1.5 Hz, 1H), 8.16 (d, *J* = 8.3 Hz, 2H), 7.70 (ddd, *J* = 8.6, 7.1, 1.6 Hz, 1H), 7.59 (d, *J* = 8.3 Hz, 1H), 7.45 - 7.38 (m, 1H), 7.35 (d, *J* = 8.2 Hz, 2H), 6.99 (s, 1H), 2.44 (s, 3H). $^{13}C\{^1H\}$ NMR (101 MHz, $CDCl_3$) δ 173.3, 155.4, 145.3, 140.6, 138.1, 133.5, 129.4, 128.3, 127.7, 125.4, 124.5, 120.7, 118.3, 21.6. HRMS (ESI) m/z: $[M-H]^-$ calcd for $C_{16}H_{11}O_3$ 251.0703; found 251.0708.

2-(4-(Dimethylamino)phenyl)-3-hydroxy-4H-chromen-4-one (C$_{26}$): Yellow solid; yield: 87%; mp: 184-186 °C (EtOH-H_2O); ^1H NMR (400 MHz, $CDCl_3$) δ 8.26 - 8.16 (m, 3H), 7.69 - 7.62 (m, 1H), 7.56 (d, *J* = 8.4 Hz, 1H), 7.38 (t, *J* =7.5 Hz, 1H), 6.92 (s, 1H), 6.81 (d, *J* = 8.0 Hz, 2H), 3.07 (s, 6H). $^{13}C\{^1H\}$ NMR (101 MHz, $CDCl_3$) δ 172.5, 155.1, 151.4, 146.7, 137.0, 132.8, 129.2, 125.2, 124.2, 120.9, 118.2, 118.0, 111.5, 40.1. HRMS (ESI) m/z: $[M-H]^-$ calcd for $C_{17}H_{14}NO_3$ 280.0969; found 280.0962.

3-Hydroxy-2-(4-Methoxyphenyl)-4H-chromen-4-one (C$_{27}$): Yellow solid; yield: 89%; mp: 232-234 °C (EtOH-H_2O); ^1H NMR (400 MHz, $CDCl_3$) δ 8.27 (dd, *J* = 9.5, 2.5 Hz, 3H), 7.72 (ddd, *J* = 8.6, 7.1, 1.6 Hz, 1H), 7.61 (d, *J* = 8.5 Hz, 1H), 7.44 (t, *J* = 7.5 Hz, 1H), 7.08 (dd, *J* = 9.5, 2.5 Hz, 2H), 3.93 (s, 3H). $^{13}C\{^1H\}$ NMR (101 MHz, $CDCl_3$) δ 173.1, 161.1, 161.1, 155.3, 145.3, 137.6, 133.4, 129.5, 125.4, 124.4, 123.6, 120.7, 118.2, 114.1, 55.4. HRMS (ESI) m/z: $[M-H]^-$ calcd for $C_{16}H_{11}O_4$ 267.0652; found 267.0647.

3-Hydroxy-2-(4-Hydroxyphenyl)-4H-chromen-4-one (C$_{28}$): Yellow solid; yield: 86%; mp: 168-170 °C (EtOH-H_2O); ^1H NMR (400 MHz, DMSO-d_6) δ 10.13 (s, 1H), 9.38 (s, 1H), 8.12 (t, *J* = 7.5 Hz, 3H), 7.77 (dt, *J* = 15.4, 7.7 Hz, 2H), 7.46 (t, *J* = 7.1 Hz, 1H), 6.96 (d, *J* = 8.8 Hz, 2H). $^{13}C\{^1H\}$ NMR (101 MHz, DMSO-d_6) δ 173.0, 159.6, 154.8, 146.5, 138.3, 133.8, 130.0, 125.2, 124.9, 122.4, 121.8, 118.7, 115.9. HRMS (ESI) m/z: $[M+H]^+$ calcd for $C_{15}H_{11}O_4$ 255.0640; found 255.0652.

2-(4-Chlorophenyl)-3-hydroxy-4H-chromen-4-one (C$_{29}$): Yellow solid; yield: 85%; mp: 198-200 °C (EtOH-H_2O); ^1H NMR (400 MHz, $CDCl_3$) δ 8.28 - 8.19 (m, 3H), 7.72 (ddd, *J* = 8.7, 7.1, 1.7 Hz, 1H), 7.59 (d, *J* = 8.5 Hz, 1H), 7.54 - 7.48 (m, 2H), 7.43 (ddd, *J* = 8.1, 7.1, 1.0 Hz, 1H), 7.07 (s, 1H). $^{13}C\{^1H\}$ NMR (101 MHz, $CDCl_3$) δ173.4, 155.4, 143.8, 138.5, 136.2, 133.9, 129.6, 129.0, 128.9, 125.5, 124.7, 120.6, 118.3. HRMS (ESI) m/z: $[M-H]^-$ calcd for $C_{15}H_8{}^{35}ClO_3$ 271.0157; found 271.0156; $[M-H]^-$ calcd for $C_{15}H_8{}^{37}ClO_3$ 273.0127; found 273.0122.

2-(4-Bromophenyl)-3-hydroxy-4H-chromen-4-one (C$_{30}$): Yellow solid; yield: 80%; mp: 189-190 °C (EtOH-H_2O); ^1H NMR (400 MHz, $CDCl_3$) δ 8.28 (d, *J* = 8.0 Hz, 1H), 8.17 (d, *J* = 8.6 Hz, 2H), 7.75 (t, *J* = 7.8 Hz, 1H), 7.69 (d, *J* = 8.6 Hz, 2H), 7.62 (d, *J* = 8.5 Hz, 1H), 7.46 (t, *J* = 7.5 Hz, 1H), 7.09 (s, 1H). $^{13}C\{^1H\}$ NMR (101 MHz, $CDCl_3$) δ 173.4, 155.4, 143.8, 138.6, 133.9, 131.9, 130.0, 129.2, 128.9, 125.5, 124.7, 120.6, 118.3. HRMS (ESI) m/z: $[M+H]^+$ calcd for $C_{15}H_{10}{}^{79}BrO_3$ 316.9710; found 316.9735; $[M+H]^+$ calcd for $C_{15}H_{10}{}^{81}BrO_3$ 318.9732; found 318.9734.

3-Hydroxy-2-(3-Methoxyphenyl)-4H-chromen-4-one (C$_{31}$): Yellow solid; yield: 70%; mp: 130-132 °C (EtOH-H_2O); ^1H NMR (400 MHz, $CDCl_3$) δ 8.28 (dd, *J* = 8.0, 1.6 Hz, 1H), 7.91 – 7.84 (m, 2H), 7.74 (ddd, *J* = 8.5, 7.1, 1.5 Hz, 1H),7.62 (d, *J* = 8.5 Hz, 1H), 7.52 – 7.41 (m, 2H), 7.06 (dd, *J* = 8.3, 2.2 Hz, 2H), 3.93 (s, 3H). $^{13}C\{^1H\}$ NMR (101 MHz, $CDCl_3$) δ 173.5, 159.7, 155.4, 144.6, 138.6, 133.7, 132.3, 129.7, 125.5, 124.6, 120.6, 120.3, 118.3, 116.0, 113.2, 55.4. HRMS (ESI) m/z: $[M+H]^+$ calcd for $C_{16}H_{11}O_4$ 267.0652; found 267.0649.

3-Hydroxy-2-(3-Hydroxyphenyl)-4H-chromen-4-one (C$_{32}$): Yellow solid; yield: 91%; mp: 235-237 °C (EtOH-H_2O); ^1H NMR (400 MHz, DMSO-d_6) δ 9.75 (s, 1H), 9.59 (s, 1H), 8.13 (dd, *J* = 8.0, 1.4 Hz, 1H), 7.85 - 7.78 (m, 1H), 7.75 (d, *J* = 8.3 Hz, 1H), 7.72 - 7.64 (m, 2H), 7.51 - 7.45 (m, 1H), 7.37 (t, *J* = 8.0 Hz, 1H), 6.92 (ddd, *J* = 8.1, 2.4, 0.8 Hz, 1H). $^{13}C\{^1H\}$ NMR (101 MHz, DMSO-d_6) δ 173.4, 157.7, 155.0, 145.7, 139.5, 134.2, 132.9, 130.0, 125.3, 125.0, 121.7, 118.9, 118.8, 117.5, 115.0. HRMS (ESI) m/z: $[M+H]^+$ calcd for $C_{15}H_{11}O_4$ 255.0650; found 255.0652.

3-Hydroxy-2-(3,4,5-Trimethoxyphenyl)-4H-chromen-4-one (C$_{33}$): Yellow solid; yield: 74%; mp: 180-182 °C (EtOH-H_2O); ^1H NMR(400 MHz, $CDCl_3$) δ 8.26 (dd, *J* = 8.0, 1.5 Hz, 1H), 7.72 (ddd, *J* = 8.6, 7.1, 1.6 Hz, 1H), 7.61 (d, *J* =8.4 Hz, 1H), 7.55 (s, 2H), 7.46 – 7.40 (m, 1H), 7.04 (s, 1H), 3.98 (s, 6H), 3.94 (s, 3H). $^{13}C\{^1H\}$ NMR (101 MHz, $CDCl_3$) δ 173.3, 155.3, 153.3, 144.7, 140.0, 138.2, 133.6, 126.3, 125.5, 124.6, 120.6, 118.3, 105.5, 61.0, 56.3. HRMS (ESI) m/z: $[M-H]^-$ calcd for $C_{18}H_{15}O_6$ 327.0864; found 327.0868.

3-Hydroxy-2-(Thiophen-2-yl)-4H-chromen-4-one (C$_{34}$): Yellow solid; yield: 75%; mp: 201-203 °C (EtOH-H_2O); ^1H NMR (400 MHz, $CDCl_3$) δ 8.27 (d, *J* = 8.0 Hz, 1H), 8.05 (d, *J* = 3.7 Hz, 1H), 7.72 (t, *J* = 7.7 Hz, 1H), 7.65 (d, *J* = 5.0 Hz, 1H), 7.60 (d, *J* = 8.5 Hz, 1H), 7.44 (t, *J* = 7.5 Hz, 1H), 7.28 – 7.21 (m, 1H), 7.11 (s, 1H). $^{13}C\{^1H\}$ NMR (101 MHz, $CDCl_3$) δ 172.5, 155.0, 142.6, 136.3, 133.5, 132.9, 129.9, 129.5, 128.1, 125.4, 124.6, 121.0, 118.2. HRMS (ESI) m/z: $[M+H]^+$ calcd for $C_{13}H_9O_3S$ 245.0267; found 245.0278.

3-Hydroxy-7-methoxy-2-phenyl-4H-chromen-4-one (C$_{35}$): Yellow solid; yield: 72%; mp: 180-182 °C (EtOH-H_2O); ^1H NMR (400 MHz, $CDCl_3$) δ 8.26 - 8.21 (m, 2H), 8.14 (d, *J* = 8.9 Hz, 1H), 7.57 - 7.41 (m, 3H), 7.08 - 6.94 (m, 3H), 3.94 (s, 3H). $^{13}C\{^1H\}$ NMR (101 MHz, $CDCl_3$) δ 172.8, 164.3, 157.4, 144.2, 138.1, 131.2, 129.9, 128.6, 127.5, 126.8, 114.9, 114.6, 99.9, 77.3, 77.0, 76.7, 55.9. HRMS (ESI) m/z: $[M-H]^-$ calcd for $C_{16}H_{11}O_4$ 267.0652; found 267.0647.

3-Hydroxy-7-methoxy-2-(4-methoxyphenyl)-4H-chromen-4-one (C$_{36}$): Brown solid; yield: 76%; mp: 192-193 °C (EtOH-H_2O); ^1H NMR (400 MHz, $CDCl_3$) δ 8.22 (d, *J* = 7.6 Hz, 2H), 8.14 (d, *J* = 8.8 Hz, 1H), 7.16 - 6.96 (m, 4H), 3.95 (s, 3H), 3.91 (s, 3H). $^{13}C\{^1H\}$ NMR (101 MHz, $CDCl_3$) δ 172.6, 164.1, 160.8, 157.2, 144.6, 137.3, 129.2, 126.7, 123.7, 114.7, 114.0, 99.8, 55.8, 55.4. HRMS (ESI) m/z: $[M+H]^+$ calcd for $C_{17}H_{15}O_5$ 229.0903; found 229.0914.

3-Hydroxy-7-methoxy-2-(4-hydroxyphenyl)-4H-chrom en-4-one (C$_{37}$): Yellow solid; yield: 85%; mp: 277-279 °C (EtOH-H_2O); ^1H NMR (400 MHz, DMSO-d_6) δ 8.11 (d, *J* = 7.7 Hz, 2H), 7.69 (d, *J* = 8.6 Hz, 1H), 7.44 (s, 1H), 7.38 (d, *J* = 8.1 Hz, 1H), 6.95 (d, *J* = 7.8 Hz, 2H), 3.88 (s, 3H). $^{13}C\{^1H\}$ NMR (101 MHz, DMSO-d_6) δ 172.5, 159.5, 156.3, 149.8, 146.4, 137.9, 130.0, 123.5, 122.5, 122.3, 120.3, 115.9, 104.3, 56.1. HRMS (ESI) m/z: $[M+H]^+$ calcd for $C_{16}H_{13}O_5$ 285.0760; found 285.0757.

3-Hydroxy-6-methoxy-2-phenyl-4H-chromen-4-one (C$_{38}$): Yellow solid; yield: 75%; mp: 204-206 °C (EtOH-H_2O); ^1H NMR (400 MHz, $CDCl_3$) δ 8.25 (d, *J* = 7.4 Hz, 2H), 7.60 – 7.43 (m, 5H), 7.31 (dd, *J* = 9.2, 3.1 Hz, 1H), 7.05 (s, 1H),3.92 (s, 3H). $^{13}C\{^1H\}$ NMR (101 MHz, $CDCl_3$) δ 173. 2, 156.5, 150.6, 144.8, 138.2, 131.2, 130.1, 128.6, 127.7, 124.5, 121.1, 119.8, 103.8, 56.0. HRMS (ESI) m/z: $[M-H]^-$ calcd for $C_{16}H_{11}O_4$ 267.0652; found 267.0649.

3-Hydroxy-6-methoxy-2-(4-hydroxyphenyl)-4H-chrom-en-4-one (C$_{39}$): Brown solid; yield: 81%; mp: 278-280 °C (EtOH-H_2O); ^1H NMR (400 MHz, DMSO-d_6) δ 10.03 (s, 1H), 9.27 (s, 1H), 8.11 (d, *J* = 8.9 Hz, 2H), 7.98 (d, *J* = 8.9 Hz, 1H), 7.24 (d, *J* = 2.3 Hz, 1H), 7.03 (dd, *J* = 8.9, 2.3 Hz, 1H), 6.95 (d, *J* = 8.9 Hz, 2H). $^{13}C\{^1H\}$ NMR (101 MHz, DMSO-d_6) δ 172.4, 163.9, 159.3, 156.7, 145.8, 137.9, 129.7, 126.5, 122.6, 115.8, 115.6, 114.9, 100.7, 56.5. HRMS (ESI) m/z: $[M+H]^+$ calcd for $C_{16}H_{13}O_5$ 285.0760; found 285.0757.

6-Fluoro-3-hydroxy-2-phenyl-4H-chromen-4-one (C$_{40}$): Yellow solid; yield: 78%; mp: 164-166 °C (EtOH-H_2O); ^1H NMR (400 MHz, $CDCl_3$) δ 8.24 (d, *J* = 7.9 Hz, 2H), 7.88 (dd, *J* = 8.0,

3.0 Hz, 1H), 7.66 – 7.40 (m, 5H), 7.01 (s, 1H). $^{13}C\{^1H\}$ NMR (101 MHz, $CDCl_3$) δ 172.9 (d, *J* = 2.7 Hz), 159.1 (d, *J* = 246.6 Hz), 151.8, 145.4, 138.2, 130.8, 130.4, 128.7, 127.8, 122.3 (d, *J* = 25.9 Hz), 121.6 (d, *J* = 8.1 Hz), 120.5 (d, *J*= 8.3 Hz), 109.9 (d, *J* = 23.7 Hz). HRMS (ESI) m/z: $[M-H]^-$ calcd for $C_{15}H_8FO_3$ 255.0452; found 255.0455.

6-Chloro-3-hydroxy-2-phenyl-4H-chromen-4-one (C_{41}): Yellow solid; yield: 81%; mp: 162-164 °C (EtOH-H_2O); ^1H NMR (400 MHz, $CDCl_3$) δ 8.26 – 8.20 (m, 3H), 7.65 (dd, *J* = 9.0, 2.6 Hz, 1H), 7.59 – 7.46 (m, 4H), 7.00 (s, 1H). $^{13}C\{^1H\}$ NMR (101 MHz, $CDCl_3$) δ 172.4, 153.7, 145.4, 138.6, 133.9, 130.7, 130.5, 130.5, 128.7, 127.8, 124.7, 121.6, 120.0. HRMS (ESI) m/z: $[M-H]^-$ calcd for $C_{15}H_8{}^{35}ClO_3$ 271.0157; found 271.0151; $[M-H]^-$ calcd for $C_{15}H_8{}^{37}ClO_3$ 273.0152; found 273.0141.

6-Bromo-3-hydroxy-2-phenyl-4H-chromen-4-one (C_{42}): Yellow solid; yield: 82%; mp: 181-183 °C (EtOH-H_2O); ^1H NMR (400 MHz, $CDCl_3$) δ 8.38 (d, *J* = 2.4 Hz, 1H), 8.27 – 8.20 (m, 2H), 7.77 (dd, *J* = 9.0, 2.4 Hz, 1H), 7.60 – 7.45 (m, 4H), 7.01 (s, 1H). $^{13}C\{^1H\}$ NMR (101 MHz, $CDCl_3$) δ 172.3, 154.1, 145.4, 138.6, 136.6, 130.7, 130.5, 128.7, 128.0, 127.8, 122.0, 120.2, 117.9. HRMS (ESI) m/z: $[M-H]^-$ calcd for $C_{15}H_8{}^{79}BrO_3$ 314.9652; found 314.9655; $[M-H]^-$ calcd for $C_{15}H_8{}^{81}BrO_3$ 316.9722; found 316.9735.

2-(4-(Diethylamino)phenyl)-3-Hydroxy-6-nitro-4H-chromen-4-one (C_{43}): Yellow solid; yield: 38%; mp: 181-183 °C (EtOH-H_2O); ^1H NMR (400 MHz, DMSO-d_6) δ 9.61 (s, 1H), 8.78 (d, *J* = 2.3 Hz, 1H), 8.54 – 8.48 (m, 1H), 8.14 (d, *J* = 8.9 Hz, 2H), 7.97 (d, *J* = 9.2 Hz, 1H), 6.82 (d, *J* = 9.0 Hz, 2H), 3.45 (q, *J* = 6.6 Hz, 4H), 1.15 (t, *J* = 6.8 Hz, 6H). $^{13}C\{^1H\}$ NMR (101 MHz, DMSO-d_6) δ 171.3, 157.5, 149.3, 144.0, 137.9, 130.0, 127.4, 122.0, 121.3, 120.7, 116.7, 111.3, 44.2, 12.9. HRMS (ESI) m/z: $[M+H]^+$ calcd for $C_{19}H_{19}N_2O_5$ 355.1214; found 355.1215.

6-Bromo-2-(4-(Diethylamino)phenyl)-3-Hydroxy-4H-chromen-4-one (C_{44}): Yellow solid; yield: 45%; mp: 181-183 °C (EtOH-H_2O); ^1H NMR (400 MHz, DMSO-d_6) δ 9.32 (s, 1H), 8.14 (d, *J* = 2.1 Hz, 1H), 8.10 (d, *J* = 8.9 Hz, 2H), 7.88 (dd, *J* = 8.9, 2.1 Hz, 1H), 7.71 (d, *J* = 8.9 Hz, 1H), 6.79 (d, *J* = 9.0 Hz, 2H), 3.43 (q, *J* = 6.8, 4H), 1.14 (t, *J* = 6.9 Hz, 6H). $^{13}C\{^1H\}$ NMR (101 MHz, DMSO-d_6) δ 170.9, 153.5, 149.1, 148.1, 137.7, 135.9, 129.9, 127.0, 123.6, 121.2, 117.1, 117.0, 111.2, 44.2, 12.9. HRMS (ESI) m/z: $[M+H]^+$ calcd for $C_{19}H_{18}{}^{79}BrNO_3$ 387.0432; found 387.0470; $[M+H]^+$ calcd for $C_{19}H_{18}{}^{81}BrNO_3$ 389.0438; found 389.0442.

3,5,7-trihydroxy-2-(4-hydroxy-3-methoxyphenyl)-4H-chromen-4-one (C_{45}): Yellow solid; yield: 41%; mp: 305-307 °C (EtOH-H_2O); ^1H NMR (400 MHz, DMSO-d_6) δ 12.48 (s, 1H), 9.78 (s, 1H), 9.47 (s, 1H), 7.77 (d, *J* = 2.1 Hz, 1H), 7.70 (dd, *J* = 8.5, 2.1 Hz, 1H), 6.95 (d, *J* = 8.5 Hz, 1H), 6.49 (d, *J* = 2.1 Hz, 1H), 6.21 (d, *J* = 2.1 Hz, 1H), 3.85 (s, 2H). $^{13}C\{^1H\}$ NMR (101 MHz, DMSO-d_6) δ 176.3, 164.4, 161.1, 156.6, 149.2, 147.8, 147.1, 136.3, 122.4, 122.2, 116.0, 112.1, 103.5, 98.7, 94.1, 56.2. HRMS (ESI) m/z: $[M+H]^+$ calcd for $C_{16}H_{13}O_7$ 317.0661; found 317.0646.

3,5,7-trihydroxy-2-(3-hydroxy-4-methoxyphenyl)-4H-chromen-4-one (C_{46}): Yellow solid; yield: 64%; mp: 266-267 °C (EtOH-H_2O); ^1H NMR (400 MHz, DMSO-d_6) δ12.47 (s, 1H), 10.81 (s, 1H), 9.41 (d, *J* = 48.6 Hz, 2H), 7.70 – 7.63 (m, 2H), 7.09 (d, *J* = 8.6 Hz, 1H), 6.44 (d, *J* = 2.1 Hz, 1H), 6.21 (d, *J* = 2.1 Hz, 1H), 3.86 (s, 3H). $^{13}C\{^1H\}$ NMR (101 MHz, DMSO-d_6) δ 176.4, 164.4, 161.2, 156.6, 149.8, 146.7, 146.6, 136.6, 123.9, 120.2, 115.1, 112.3, 103.5, 98.7, 93.9, 56.1. HRMS (ESI) m/z: $[M+H]^+$ calcd for $C_{16}H_{13}O_7$ 317.0661; found 317.0632.

3,5,7-trihydroxy-2-(4-methoxyphenyl)-4H-chromen-4-one (C_{47}): Yellow solid; yield: 65%; mp: 276-277 °C (EtOH-H_2O); ^1H NMR (400 MHz, DMSO-d_6) δ 12.47 (s, 1H), δ 10.86 (s, 1H) 9.56 (s, 1H), 8.15 (d, *J* = 8.9 Hz, 1H), 7.12 (d, *J* = 8.9 Hz, 1H), 6.47 (d, *J* = 1.7 Hz, 1H), 6.21 (d, *J* = 1.7 Hz, 1H), 3.85 (s, 2H). $^{13}C\{^1H\}$ NMR (101 MHz, DMSO-d_6) δ 176.5, 164.4, 161.2, 160.9, 156.7, 146.7, 136.5, 129.8, 123.7, 114.5, 103.6, 98.7, 94.0, 55.8. HRMS (ESI) m/z: $[M+H]^+$ calcd for $C_{16}H_{13}O_6$ 301.0712; found 301.0723.

(Z)-2-(4-Bromobenzylidene)-4-Methoxybenzofuran-3(2H)-one (D_7) Yellow solid; yield: 75%; mp: 161-164 °C (EtOH-H_2O); ^1H NMR (400 MHz, $CDCl_3$) δ 7.78 (d, *J* = 8.5 Hz, 2H), 7.59 (m, 3H), 6.91 (d, *J* = 8.2 Hz, 1H), 6.78 (s, 1H), 6.66 (d, *J* = 8.3 Hz, 1H), 4.03 (s, 3H). $^{13}C\{^1H\}$ NMR (101 MHz, CDCl3) δ 167.0, 158.6, 147.1, 138.6, 132.6, 132.1, 131.4, 124.0, 110.5, 105.4, 104.8, 56.3. HRMS (ESI) m/z: $[M+Na]^+$ calcd for $C_{16}H_{11}{}^{79}BrNaO_3$ 352.9789; found 352.9784; $[M+Na]^+$ calcd for $C_{16}H_{11}{}^{81}BrNaO_3$ 354.9769; found 352.9784.

(Z)-4-Methoxy-2-(4-Nitrobenzylidene)benzofuran-3(2H)-one (D_8): Yellow solid; yield: 81%; mp: 170-173 °C (EtOH-H_2O); ^1H NMR (400 MHz, $CDCl_3$) δ 8.31 (d, *J* = 8.8 Hz, 2H), 8.06 (d, *J* = 8.8 Hz, 2H), 7.66 (t, *J* = 8.3 Hz, 1H), 6.94 (d, *J* = 8.2 Hz, 1H), 6.85 (s, 1H), 6.70 (d, *J* = 8.4 Hz, 1H), 4.05 (s, 3H). $^{13}C\{^1H\}$ NMR (101 MHz, DMSO) δ 164.6, 136.2, 135.7, 134.1, 132.7, 131.8, 130.5, 129.5, 129.4, 129.4, 113.6, 67.4. HR-ESIMS: 298.0637; $[M+H]^+$ (calc. for $C_{16}H_{12}NO_5$, 298.0715).

(Z)-2-(4-Hydroxy-3,5-Dimethoxybenzylidene)-4-Methoxybenzofuran-3(2H)-one (D_{13}): Yellow solid; yield: 30%; mp: 160-162 °C ^1H NMR (400 MHz, $CDCl_3$) δ 7.59 (t, *J* = 8.0 Hz, 1H) 7.22 (s, 2H), 7.00 (d, *J* = 8.8 Hz, 1H), 6.81 (s, 1H), 6.58 (dd, *J* = 17.5, 8.3 Hz, 1H), 3.93 (s, 1H), 3.86 (s, 2H). $^{13}C\{^1H\}$ NMR (101 MHz, MeOD) δ 195.1, 162.0, 161.8, 160.3, 143.8, 141.0, 134.3, 130.0, 127.7, 125.1, 114.1, 113.0, 109.6, 101.8, 55.1, 54.5. HRMS (ESI) m/z: $[M+Na]^+$ calcd for $C_{18}H_{16}NaO_6$ 351.0845; found 351.0839.

(E)-1-(2-hydroxy-6-methoxyphenyl)-3-(4-methoxyphenyl)prop-2-en-1-one (Y_1): Yellow solid; yield: 82%; ^1H NMR (400 MHz, CD_3OD) δ 7.70 – 7.52 (m, 4H), 7.37 (t, *J* = 8.3 Hz, 1H), 7.00 (d, *J* = 8.8 Hz, 1H), 6.58 (dd, *J* = 17.5, 8.3 Hz, 1H), 3.93 (s, 1H), 3.86 (s, 2H). $^{13}C\{^1H\}$ NMR (101 MHz, CD_3OD) δ 195.1, 162.0, 161.8, 160.3, 143.8, 141.0, 134.3, 130.0, 127.7, 125.1, 114.1, 113.0, 109.6, 101.8, 55.1, 54.5. HRMS (ESI) m/z: $[M+H]^+$ calcd for $C_{17}H_{17}O_4$ 285.1052; found 285.1048.

3-hydroxy-5-methoxy-2-(4-methoxyphenyl)chroman-4-one (V_1): White solid; yield: 46%; ^1H NMR (400 MHz, CD_3OD) δ 7.54 – 7.41 (m, 3H), 7.00 (d, *J* = 8.8 Hz, 2H), 6.72 (d, *J* = 8.4 Hz, 1H), 6.62 (d, *J* = 8.4 Hz, 1H), 5.08 (d, *J* = 11.9 Hz, 1H), 4.54 (d, *J* = 12.0 Hz, 1H), 3.92 (s, 2H), 3.85 (s, 1H). $^{13}C\{^1H\}$ NMR (101 MHz, CD_3OD) δ 193.2, 162.9, 160.7, 160.2, 136.7, 129.1, 128.8, 113.4, 109.5, 103.9, 100.0, 83.0, 73.4, 55.1, 54.4. HRMS (ESI) m/z: $[M+H]^+$ calcd for $C_{17}H_{17}O_5$ 301.1012; found 301.0998.

5-methoxy-2-(4-methoxyphenyl)chroman-4-one (Z_1): Yellow solid; yield: 35%; ^1H NMR (400 MHz, CD_3OD) δ 7.44 (d, *J* = 8.7Hz, 1H), 6.98 (d, *J* = 8.7Hz 1H), 6.67 (dd, *J* = 11.9, 8.4 Hz, 1H), 5.44 (dd, *J* = 12.9, 2.9 Hz, 1H), 3.89 (s, 2H), 3.83 (s, 2H), 3.13 (dd, *J* = 16.6, 12.9 Hz, 1H), 2.78 (dd, *J* = 16.6, 3.0 Hz, 1H). $^{13}C\{^1H\}$ NMR (101 MHz, CD_3OD) δ 192.2, 163.5, 160.8, 160.0, 136.4, 130.9, 127.5, 113.6, 110.7, 109.8, 103.8, 78.6, 55.0, 54.4, 45.2. HRMS (ESI) m/z: $[M+H]^+$ calcd for $C_{17}H_{17}O_4$ 285.1056; found 285.1049.

(Z)-4-methoxy-2-(4-methoxybenzylidene)benzofuran-3(2H)-one (D_1): Yellow needles; yield: 85%; ^1H NMR (400 MHz, $CDCl_3$) δ 7.97 – 7.83 (m, 2H), 7.65 – 7.49 (m, 1H), 7.08 – 6.95 (m, 2H), 6.94 – 6.73 (m, 2H), 6.63 (d, *J* = 8.3 Hz, 1H), 4.03 (s, 3H), 3.89 (s 3H). $^{13}C\{^1H\}$ NMR (101 MHz, $CDCl_3$) δ 182.3, 166.8, 160.8, 158.5, 145.9, 138.0, 133.2, 125.2, 114.4, 112.2, 111.2, 104.9, 104.8, 56.3, 55.4. HRMS (ESI) m/z: $[M+H]^+$ calcd for $C_{17}H_{15}O_4$ 283.0965; found 283.0967.

■ ASSOCIATED CONTENT

Supporting Information. The Supporting Information is available free of charge on the ACS Publications website.
Experimental details, spectroscopic data and analytical data (PDF)

■ AUTHOR INFORMATION

Corresponding Author

* wangchun@cib.ac.cn
* zhanggl@cib.ac.cn

ORCID[ID]*:*

Chun Wang: 0000-0001-8553-1182

Present Addresses

†If an author's address is different than the one given in the affiliation line, this information may be included here.

Author Contributions

‖ Wei Xiong and Xiaohong Wang contributed equally.

Funding Sources

Any funds used to support the research of the manuscript should be placed here (per journal style).

Notes

The authors declare no competing financial interest.

■ ACKNOWLEDGMENT

Financial supports from the National Natural Science Foundation of China (No. 21561142003 and No. 21977092), the National New Drug Innovation Major Project of China (2018ZX09711001-001-006), and Science and Technology Department of Sichuan Province (2019YFS0106), are gratefully acknowledged.

■ REFERENCES

(1) (a) Huang, Z. L.; Jing, X. Q.; Sheng, Y. S.; Zhang, J. Q.; Hao, Z.; Wang, Z. T.; Ji, L. L. (-)-Epicatechin attenuates hepatic sinusoidal obstruction syndrome by inhibiting liver oxidative and inflammatory injury. *Redox Biol.* **2019**, *22*, 101-117. (b) Zhang, S. D.; Wang, P.; Zhang, J.; Wang, W.; Yao, L. P.; Gu, C. B.; Efferth, T.; Fu, Y. J. 2'-O-galloylhyperin attenuates LPS-induced acute lung injury via up-regulation antioxidation and inhibition of inflammatory responses in vivo. *Chem. Biol. Interact.* **2019**, *304*, 20-27. (c) Jian, J.; Fan, J. L.; Yang, H.; Lan, P.; Li, M. M.; Liu, P. J.; Gao, H.; Sun, P. H. Total synthesis of the flavonoid natural product houttuynoid A. *J. Nat. Prod.* **2018**, *81*, 371-377. (d) Wang, J. Q.; Wang, X. B.; Wang, Y.; Tang, W. J.; Shi, J. B.; Liu, X. H. Novel curcumin analogue hybrids: synthesis and anticancer activity. *Eur. J. Med. Chem.* **2018**, *156*, 493-509.

(2) Brusselmans, K.; Vrolix, R.; Verhoeven, G.; Swinnen, J. V. Induction of cancer cell apoptosis by flavonoids is associated with their ability to inhibit fatty acid synthase activity. *J. Biol. Chem.* **2005**, *280*, 5636-5645.

(3) Zhao, H.; Guo, Y. M.; Li, S.; Han, R. Q.; Ying, J. M.; Zhu, H.; Wang, Y. Y.; Yin, L.; Han, Y. Q.; Sun, L. Z.; Wang, Z. Y.; Lin, Q. C.; Bi, X. Y.; Jiao, Y. C.; Jia, H. Y.; Zhao, J. J.; Huang, Z.; Li , Z. Y.; Zhou, J. G.; Song, W.; Meng, K.; Cai, J. Q. A novel anti-cancer agent Icaritin suppresses hepatocellular carcinoma initiation and malignant growth through the IL-6/Jak2/Stat3 pathway. *Oncotarget* **2015**, *6*, 31927-31943.

(4) Xu, M.; Pirtskhalava, T.; Farr, J. N.; Weigand, B. M.; Palmer, A. K.; Weivoda1, M. M.; Inman, C. L.; Ogrodnik, M. B.; Hachfeld, C. M.; Fraser, D. G.; Onken, J. L.; Johnson, K. O.; Verzosa, G. C.; Langhi, L. G. P.; Weigl, M.; Giorgadze, N.; LeBrasseur, N. K.; Miller, J. D.; Jurk, D.; Singh, R. J.; Allison, D. B.; Ejima, K.; Hubbard, G. B.; Ikeno, Y. J.; Cubro, H.; Garovic, V. D.; Hou, X. N.; Weroha, S. J.; Robbins, P. D.; Niedernhofer, L. J.; Khosla, S.; Tchkonia1, T.; Kirkland, J. L. Senolytics improve physical function and increase lifespan in old age. *Nature Med.* **2018**, *24*, 1246-1256.

(5) (a) Algar, J.; Flynn, J. P. A new method for the synthesis of flavonols. *Proc. R. Ir. Acad.* **1934**, *42*, 1-8. (b) Taichiro, O. A new generalmethod for the synthesis of the derivatives of flavonol. *J. Chem. Soc. Japan* **1935**, *10*, 182-186. (c) Gunduz, S.; Goren, A. C.; Ozturk, T. Facile syntheses of 3-hydroxyflavones. *Org. Lett.* **2012**, *14*, 1576-1579.

(6) (a) Mahal, H. S.; Venkataraman, K. Synthetical experiments in the chromone group. Part XIV. The action of sodamide on 1-acyloxy-2-acetonaphthones. *J. Chem. Soc.* **1934**, 1767-1769. (b) Bois, F.; Beney, C.; Mariotte, A. M.; Boumendjel, A. A one-step synthesis of 5-hydroxyflavones. *Synlett.* **1999**, *1999*, 1480-1482. (c) Ganguly, A. K.; Kaur, S.; Mahata, P. K.; Biswas, D.; Pramanik, B. N.; Chan, T. M. Synthesis and properties of 3-acyl- γ -pyrones, a novel class of flavones and chromones. *Tetrahedron Lett.* **2005**, *46*, 4119-4121.

(7) Auwers, K.; Müller, K. Umwandlung von benzal-cumaranonen in flavonole. *Eur. J. Inorg. Chem.* **1908**, *41*, 4233-4241.

(8) (a) Adam, W.; Golsch, D.; Hadjiarapoglou, L. Epoxidation of flavones by dimethyldioxirane. *J. Org. Chem.* **1991**, *56*, 7292-7297. (b) Li, S.; Pan, M. H.; Lai, C. S.; Lo, C. Y.; Dushenkov, S.; Ho, C. T. Isolation and syntheses of polymethoxyflavones and hydroxylated polymethoxyflavones as inhibitors of HL-60 cell lines. *Bioorg. Med. Chem.* **2007**, *15*, 3381-3389. (c) Chu, H. W.; Wu, H. T.; Lee, Y. J. Regioselective hydroxylation of 2-hydroxychalcones by dimethyldioxirane towards polymethoxylated flavonoids. *Tetrahedron* **2004**, *60*, 2647-2655.

(9) Adams, C. J.; Main, L. Cyclisation and subsequent reactions of 2'-hydroxy-6'-methoxychalcone epoxide and related compounds. *Tetrahedron* **1991**, *47*, 4979-4990.

(10) (a) Sundén, H.; Ibrahem, I.; Zhao, G. L.; Eriksson, L.; Cordova, A. Catalytic enantioselective domino oxa-michael/aldol condensations: asymmetric synthesis of benzopyran derivatives. *Chem. Eur. J.* **2007**, *13*, 574-581. (b) Zhang, F. L.; Xu, A. W.; Gong, Y. F.; Wei, M. H.; Yang, X. L. Asymmetric organocatalytic four-component quadruple domino reaction initiated by oxa-michael addition of alcohols to acrolein. *Chem. Eur. J.* **2009**, *15*, 6815-6818. (c) Lu, L. Q.; Chen, J. R.; Xiao, W. J. Development of cascade reactions for the concise construction of diverse heterocyclic architectures. *Acc. Chem. Res.* **2012**, *45*, 1278-1293.

(11) Torre, A. F. D. L.; Rivera, D. G.; Ferreira, M. A. B. Corrêa, A. G.; Paixão, M. W. Multicomponent combinatorial development and conformational analysis of prolyl peptide-peptoid hybrid catalysts: application in the direct asymmetric michael addition. *J. Org. Chem.* **2013**, *78*, 10221-10232.

(12) (a) Cai, X. L.; Chang, V.; Chen, C. F.; Kim, H. J.; Mariano, P. S. A potentially general method to control relative stereochemistry in enone-olefin [2+2]-photocycloaddition reactions by using eniminium salt surrogates. *Tetrahedron Lett.* **2000**, *41*, 9445-9449. (b) Chen, C. F.; Chang, V.; Cai, X. L.; Duesler, E.; Mariano, P. S. A general strategy for absolute stereochemical control in enone-olefin [2+2] photocycloaddition reactions. *J. Am. Chem. Soc.* **2001**, *123*, 6433-6434. (c) Hörmann, F. M.; Chung, T. S.; Rodriguez, E.; Jakob, M.; Bach, T. Evidence for triplet sensitization in the visible-light-induced [2+2] photocycloaddition of eniminium ions. *Angew. Chem. Int. Ed.* **2018**, 57, 827-831.

(13) (a) Gotoh, H.; Hayashi, Y. J. Diarylprolinol silyl ether as catalyst of an exo-selective, enantioselective Diels-Alder reaction. *Org. Lett.* **2007**, *9*, 2859-2862. (b) Hayashi, Y. J.; Samanta, S.; Gotoh, H.; Ishikawa, H. Asymmetric Diels-Alder reactions of a,b-unsaturated

aldehydes catalyzed by a diarylprolinol silyl ether salt in the presence of water. *Angew. Chem. Int. Ed.* **2008**, *47*, 6634-6637.

(14) Silvi1, M.; Verrier, C.; Rey, Y. P.; Buzzetti, L. Melchiorre, P. Visible-light excitation of iminium ions enablesthe enantioselective catalytic β-alkylation of enals. *Nat. Chem.* **2017**, *9*, 868-873.

(15) Davis, R. L.; Jensen, K. L.; Gschwend, B.; Jørgensen, K. A. On the mechanism of the organocatalytic asymmetric epoxidation of *α*, *β*-unsaturated aldehydes. *Chem. Eur. J.* **2014**, *20*, 64-67.

(16) (a) Ghogare, A. A.; Greer, A. Using singlet oxygen to synthesize natural products and drugs. *Chem. Rev.* **2016**, *116*, 9994-10034. (b) Baptista, M. D. S.; Cadet, J.; Mascio, P. D.; Ghogare, A. A.; Greer, A.; Hamblin, M. R.; Lorente, C.; Nunez, S. C.; Ribeiro, M. S.; Thomas, A. H.; Vignoni, M.; Yoshimura, T. M. Type I and II photosensitized oxidation reactions: guidelines and mechanistic pathways. *Photochem. Photobiol.* **2017**, *93*, 912-919.

(17) Davies, M. J. Free radicals, oxidants and protein damage. *Aust. Biochemist* **2012**, *43*, 8 -12.

(18) Ghogare, A. A.; Greer, A. Using singlet oxygen to synthesize natural products and drugs. *Chem. Rev.* **2016**, *116*, 9994-10034.

(19) Wu, Q. Q.; Wang, Z.; Li, J.; Qiu, S.; Cao, D. X.; Liu, Z. Q.; Guan, R. F. 3-Hydroxyflavone derivatives synthesized by a new simple method as chemosensors for cyanide anions. *RSC Adv.* **2016**, *6*, 72698-72702.

(20) (a) Bouktaib, M.; Lebrun, S.; Atmani, A.; Rolando, C. Hemisynthesis of all the O-monomethylated analogues of quercetin including the major metabolites, through selective protection of phenolic functions. *Tetrahedron* **2002**, *58*, 10001-10009. (b) Pandurangan, N.; Bose, C.; Banerji, A. Synthesis and antioxygenic activities of seabuckthorn flavone-3-ols and analogs. *Bioorg. Med. Chem. Lett.* **2011**, *21*, 5328-5330. (c) Kato, K.; Ninomiya, M.; Tanaka, K.; Koketsu, M. Effects of functional groups and sugar composition of quercetin derivatives on their radical scavenging properties. *J. Nat. Prod.* **2016**, *79*, 1808-1814.

(21) Reisinger, C. M.; Wang, X. W.; List, B. Catalytic asymmetric hydroperoxidation of alpha,beta-unsaturated ketones: an approach to enantiopure peroxyhemiketals, epoxides, and aldols. *Angew. Chem. Int. Ed.* **2008**, *47*, 8112-8115.

(22) Zou, L., Yan, B., Pan, D., Tan, Z. Bao, X. P. A colorimetric and absorption ratiometric anion sensor based on indole & hydrazide binding units. *Spectro. Acta Part A Molecular & Biomol. Spectro.,* **2015**, *148*, 78-84.

(23) Silverman, S. K.; Foote, C. S. Singlet oxygen and electron-transfer mechanisms in the dicyanoanthracene-sensitized photooxidation of 2,3-diphenyl-1,4-dioxene. *J. Am. Chem. Soc.* **1991**, *113*, 7672-7675.

(24)Wang, Y. T.; Jin, K. J.; Leopold, S. H. Wang, J.; Peng, H. L.; Platz, M. S.; Xue, J.; Phillips, D. L.; Glover, S. A.; Novak, M. Characterization of reactive intermediates generated during photolysis of 4-acetoxy-4-aryl-2,5-cyclohexadienones: oxenium ions and aryloxy radicals. *J. Am. Chem. Soc.* **2008**, *130*, 16021-16030.

(25) Baptista, M. D. S.; Cadet, J.; Mascio, P. D.; Ghogare, A. A.; Greer, A.; Hamblin, M. R.; Lorente, C.; Nunez, S. C.; Ribeiro, M. S.; Thomas, A. H.; Vignoni, M.; Yoshimura, T. M. Type I and II photosensitized oxidation reactions: guidelines and mechanistic pathways. *Photochem. Photobiol.* **2017**, *93*, 912-919.

(26) (a) Schmidt, R.; Afshari, E. Collisional deactivation of O_2 ($^1\triangle$ g) by solvent molecules comparative experiments with $^{16}O_2$ and $^{18}O_2$. *Ber. Bunsenges. Phys. Chem.* **1992**, *96*, 788-794. (b) Schweitzer, C.; Schmidt, R. Physical mechanisms of generation and deactivati of singlet oxygen. *Chem. Rev.* **2003**, *103*, 1685-1757.

(27) M. J. Frisch, et al. Gaussian 03, Revision D. 01, Gaussian, Inc., Wallingford CT, 2004.

(28) Zhao, Y.; Truhlar, D. G. The M06 suite of density functionals for main group thermochemistry, thermochemical kinetics, noncovalent interactions, excited states, and transition elements: two new functionals and systematic testing of four M06-class functionals and 12 other functionals. *Theor. Chem. Acc.* **2008**, *120*, 215-241.

(29) (a) Mennucci, B.; Tomasi, J. Continuum solvation models: A new approach to the problem of solute's charge distribution and cavity boundaries. *J. Chem. Phys.* **1997**, *106*, 5151-5158. (b) Mennucci, B.; Cancès, E. Tomasi J . Evaluation of solvent effects in isotropic and anisotropic dielectrics and in ionic solutions with a unified integral equation method: theoretical bases, computational implementation, and numerical applications. *J. Phys. Chem. B* **1997**, *101*, 10506-10517. (c) Tomasi, J.; Mennucci, B.; Cancès, E.. The IEF version of the PCM solvation method: An overview of a new method addressed to study molecular solutes at the QM ab initio level. *J Mol Struct (THEOCHEM)*, **1999**, *464*, 211-226.